



Politecnico di Milano

School of Industrial and Information Engineering

Degree Course of Master of Science in Mechanical Engineering

**Effects of Topology Optimisation and Infill Density on
Mechanical Properties of Extrusion Based Additive
Manufacturing Samples**

Thesis Supervisor: Prof. Ing. Matteo Strano

Co-Supervisor: Ing. Kedarnath Rane

Master's thesis by:

Hambal Iqbal (ID: 10598346)

Academic Year 2017 – 2018

Acknowledgment

I am pleased to extend my special thanks to my supervisor, **Professor Matteo Strano** who has been a great help throughout the length of this work. His guidance and expert advices have enabled me to finish this thesis timely and efficiently. He has invested invaluable support and greatly responded to all my queries in no time. I am obliged to have worked under the supervision of a highly calibre professor.

Moreover, I would like to acknowledge the contributions of Postdoctoral Researcher **Kedarnath Rane** who put his constant efforts to introduce scientific and technical aspects which helped me greatly towards a more diverse work.

Furthermore, I would like to thank the Faculty of Industrial and Information Engineering at Politecnico di Milano for providing me with state-of-the-art facilities and machineries to uplift the research outputs.

Eventually, I dedicate this thesis to my parents.

HAMBAL IQBAL

Milan, March 2021

Abstract

The world is proceeding towards mass customization due to the increasing individual demands of end-users. Consequently, manufacturing systems must show adaptability to meet the changing consumer needs. As a result, specific methods with certain tools and strategies should be brought into practice to globalize the mass customization. Mass customization facilitates in manufacturing products, specific to customers, as per individual needs but traditional manufacturing faces severe challenges to implement mass customization due to the traditional approach of design for manufacturing. Alternatively, additive manufacturing has proved to be the best technology to provide mass customization solutions with even more complex and customer specific products. Moreover, design for additive manufacturing (DFAM) parts can be produced with short lead time with comparable strength to those produced with traditional manufacturing approaches. Thus, additive manufacturing can be more diverse and applicable towards mass customization solutions. This work is presented to evaluate different mass reduction strategies by combined effects of topology optimization and infill density for extrusion based additive manufacturing and study their strength with respect to their manufacturing time (cost). The study is carried out on bio-degradable PLA, manufactured using Fused Deposition Modeling (FDM). The experimental analysis is carried out with standard compression and tensile specimens for 5 levels of mass retained i.e. 100%, 85%, 70%, 50% and 30%. Mass reduction is done by the combination of topology optimization and infill density, using a proportion of 50:50, 33:67 and 66:34. Therefore, 5 different levels for both compression and tensile specimens and 3 levels of crosshead speed (0.25, 2.5 and 25 mm/min), 78 specimens were tested. The additive manufacturing of these specimens was performed on Creality Ender-3 FDM machine with preset process parameters. As a result of the experimental analysis, the mechanical properties such as young's modulus, yield strength, maximum stress induced, and cost-coefficient are verified. The results obtained from experimental analysis support the fact that all the parameters with varying levels effect the components' strength and cost-coefficient. Consequently, we can have an acceptable trade-off between the strength and manufacturing lead time/material consumed and hence cost of manufacturing.

Contents

1. Introduction	8
1.1. Additive Manufacturing	9
1.2. Process and Technology	10
1.2.1. Process chain of AM	11
1.2.2. Fused Deposition Modeling (FDM)	12
1.2.3. Benefits and Limitations of AM Technology	14
3. Topology and infill	23
3.1. Topology optimisation	24
3.1.1. Optimisation approach	24
3.2. Infill density	27
3.3. Solid and porous structures	27
3.4. Effect on strength and stiffness	28
3.5. Limitations and challenges	29
3.6. Mass customisation	30
4. Methodology	32
4.1. Tools for Topology Optimisation and Infill Density	37
4.1.1. SolidThinking Inspire and ANSYS	38
4.1.2. Ultimaker Cura	39
5. Experiments	41
5.1. Experimental Setup	42
5.2. Mechanical Testing	44
6. Results	47
6.1. Experimental Results	47
6.1.1. Compression Test	47
6.1.2. Tensile Test	55
7. Conclusion	63
8. References	65

LIST OF FIGURES:

Figure 1 Various AM processes [5]	11
Figure 2 FDM process [8].....	12
Figure 3 Honeycomb structure (left), structure (left), structure generated by topology optimisation (middle) and with local volume constraints (right) [9].....	17
Figure 4 Self-supporting rhombic infill structure that are refined adaptively (left), and uniformly (middle) and structure generated by local volume constrained topology optimisation (right) [9].....	17
Figure 5 Influence of build orientation and extrusion path on the strength [11]	18
Figure 6 Dependence of tensile strength on the actual volume fraction of infill [14]	19
Figure 7 Tracks' interaction of different theoretical volume fractions of the infill structure: 40% (top), 80% (left), 100% (right) [14]	19
Figure 8 Fracture load depending on base thickness and infill density for samples with shell thickness of 1.2mm [16]	20
Figure 9 (a) Solid component (b) Porous component (c) Stiffness as a function of material density [18]	21
Figure 10 Mix of papers on additive manufacturing [27].....	22
Figure 11 3D printed samples from topology optimisation [15]	24
Figure 12 Size, shape, and continuum topology optimisation [12]	25
Figure 13 Shape optimisation path and results [15].....	27
Figure 14 Maximum force as a function of infill structure and density [21].....	29
Figure 15 Product variety-volume matrix [5]	30
Figure 16 3D mass customisation cycle [26].....	31
Figure 17 Goals and constraints panel in Solidworks 2018.....	33
Figure 18 Topology optimisation of bracket in Solidworks 2018	33
Figure 19 Density distribution of topology optimisation.....	34
Figure 20 CAD model of tensile specimen.....	35
Figure 21 Sliced sample of 70% mass: 50% topology, 50% infill	36
Figure 22 3D printed Tensile and compression specimens	37
Figure 23 Important print parameters from Cura.....	40
Figure 24 Topologically optimised parts with (a) 30%, (b) 50% and (c) 85% infill density ..	40
Figure 25 FDM Machine	41
Figure 26 Tensile specimens optimised sections during printing	41
Figure 27 50% mass reduction, 66% by topology while 34% by infill density.....	42
Figure 28 Weight measurement	43
Figure 29 Stress-strain graph of 100% dense tensile specimen	44
Figure 30 Standard for tensile test	45
Figure 31 Standard for compression test	45
Figure 32 Compression and Tensile testing machines.....	45
Figure 33 Fracture points of different tensile samples.....	46
Figure 34 Fracture points of different compression samples.....	46
Figure 35 Main effects plot of E for compression	49
Figure 36 Main effects plot of YS for compression	50
Figure 37 Main effects plot of maximum compression strength	50
Figure 38 Main effects plot of cost-coefficient for compression.....	51
Figure 39 Interaction plot of E for compression	51

Figure 40 Interaction plot of YS for compression	52
Figure 41 Main effects plot of maximum compression strength	52
Figure 42 Main effects plot of cost-coefficient for compression.....	53
Figure 43 Probability plot of compression.....	53
Figure 44 Scatter plot of SRES vs Fits, E, YS, Max compression strength	54
Figure 45 Scatterplot of Mass vs E, YS, cost-coefficient and maximum compression strength	54
Figure 46 Main effects plot of E for Tensile.....	57
Figure 47 Main effects plot of Yield Strength for Tensile.....	57
Figure 48 Main effects plot of Maximum tensile strength	58
Figure 49 Main effects plot of cost-coefficient for Tensile	58
Figure 50 Interaction plot of E for Tensile	59
Figure 51 Interaction plot of Yield Strength for Tensile	59
Figure 52 Interaction plot of Maximum Tensile Strength	60
Figure 53 Interaction plot of cost-coefficient for Tensile.....	60
Figure 54 Probability plot of Tensile	61
Figure 55 Scatter plot of SRES vs Fits, E, YS and Maximum tensile strength.....	61
Figure 56 Scatterplot of mass vs E, YS, cost-coefficient, and maximum tensile strength	62

LIST OF TABLES:

Table 1 Different materials for FDM and their properties [7]	13
Table 2 Advantages, disadvantages, and applications of various AM processes [6]	15
Table 3 Plan for mass reduction for each sample with relevant topology and infill %	36
Table 4 Different Mass reduction strategies	43
Table 5 Some random compression and tensile specimens with corresponding strategies, crosshead speeds and dimensions	44
Table 6 ANOVA of Young's Modulus for compression	48
Table 7 ANOVA of Yield Strength for compression	48
Table 8 ANOVA of Maximum Compression strength	48
Table 9 ANOVA of cost-coefficient for compression	49
Table 10 ANOVA of Young's Modulus for Tensile	55
Table 11 ANOVA of Yield Strength for Tensile	55
Table 12 ANOVA of Maximum Tensile Strength	56
Table 13 ANOVA of cost-coefficient for Tensile	56

1. Introduction

Additive Manufacturing (3D Printing) is one of the hot topics in this era which uses a digital design file and prints a solid component in a layer-wise manner. The application of this technology has extended to many fields especially aerospace, automotive and medical industries. Moreover, topology optimization has been exclusively in the research until the emergence of additive manufacturing. Topology optimization is a part design technique aimed at reducing the mass without compromising the strength while additive manufacturing has the ability to produce very less or no scrap. The combination of topology optimization and additive manufacturing has paved the way in printing customized lightweight components in various industries. There are many factors which has made additive manufacturing very important in this age of science and technology. For example, wide variety of CAD/CAM software, better equipment and component technologies, especially low-cost motion systems and high-power lasers. A vast bank of materials i.e. filaments, powders, while key industry and government initiatives with an inventive vision cumulatively helped in proceeding with this technology so fast.

Commercial slicers have their infill density reduction strategies which are generally aimed at increasing the printing speed (hence reduced manufacturing time) which is desirable for reduced cost of manufacturing. Topology optimization has the potential to reduce the weight, while maintaining the structural requirements. Moreover, in conventional manufacturing, topology may limit the manufacturability while in additive manufacturing it can have more design freedom and hence topology optimization is a key part of design for additive manufacturing.

The purpose of this work is to present the combined effects of topology optimization and conventional infill density reduction strategies on the strength and/or cost of extrusion based additive manufacturing parts. There is not much research on the combination of topology optimization and infill density to incorporate reduced mass in additive manufacturing parts. Therefore, to evaluate the objective of this work, the following steps are observed.

- a) Studying the current literature of topology optimization, infill density and their combination on the strength of FDM printed parts
- b) Examining the appropriate combination of FDM 3D printer's process parameters used for printing the mechanical test specimens (Tensile and Compression specimens)

- c) To investigate the combined effects of topology optimization and infill density on the mechanical properties of specimens in order to produce low cost, lightweight components with extrusion-based additive manufacturing technology. The most crucial optimization level and infill percentages are selected as per previous promising state of the art
- d) Designing the specimens for topology optimization based on our study under discussion
- e) Printing the designed tensile and compression specimens with preset parameters
- f) Carrying out mechanical tests for compression and tensile parts and obtaining the corresponding mechanical properties against each specimen with various topology and infill parameters
- g) Analyzing the results in statistical tool in order to find the significant level of optimization and/or their combinations

The entire process chain along-with the state of the art, experiments and discussions will be presented in the upcoming chapters in details. Following is just an overview of how this work is organized.

In the second chapter, the state of the art is covered. In this regard, efforts were made to include the most up-to-date facts and figures from the recent researchers. Moreover, an introduction in understanding of topology optimization and infill density with respect to mass customization is added in chapter three while chapter four describes the methodology used to carry out the experimental and design part. Chapter five introduces the experimental plan, setup, and mechanical testing. Chapter six and seven details the experimental results of tensile and compression tests and conclusions are drawn, respectively.

1.1. Additive Manufacturing

Additive manufacturing (AM) is defined as “a process of joining materials to make objects from 3D model data, usually layer upon layer, as opposed to subtractive manufacturing methodologies” [1]. It is probably the best technology for providing mass customization solutions to industries which are committed in providing on demand customized parts.

Moreover, AM is also resource-efficient because the products are built by growing component layers from computer-aided design (CAD) data with very little scrap or waste [2]. Due to the growing popularity and its proven capabilities, additive manufacturing is enabling a design and

industrial revolution in many sectors such as medical, energy, aerospace, automotive and many more.

1.2. Process and Technology

A 3D printer uses a raw material and a computer-aided design (CAD) file and produces a finished product. The raw material is typically in the form of powder or filament. Unlike the traditional manufacturing technology, which uses moulds and dies, this technology produces each part as unique. We just need to feed our 3D printer with a different CAD file.

Additive manufacturing is a young technology, in fact, the word “additive manufacturing” and the abbreviation “AM” dates to 2000s and there are many additive manufacturing processes and technologies from its emergence and various variants are used by different companies for the same system. For example, what the Stratasys company calls “fused deposition modelling” (FDM) is basically the same what 3D Systems calls “plastic jet printing”, where is others refer to it as “fused filament fabrication” [4]. Therefore, here we will adopt the terminology laid down by the American Society of Testing and Materials (ASTM) in 2012 which introduces seven variants because of their different methodologies and equipment used and briefly describe each process:

1. **Powder bed fusion:** Perhaps the most popular in metal 3D printing, uses a high energy laser beam for depositing metal powder selectively on a powder bed and sinters them accordingly.
2. **Vat photo-polymerization:** The oldest AM process, also called stereo-lithography, uses an ultraviolet (UV) laser to cure a UV-curable monomer dissolved in a solvent [4].
3. **Material jetting:** This process uses the droplets of thermosetting resin cured by high intensity UV light sources and deposit it layer by layer.
4. **Material extrusion:** In this process a filament is extruded in a heated nozzle and is deposited layer by layer on a heated bed (build plate). The process is detailed in the next section.

5. **Sheet lamination:** Its input is a roll or stack of thin sheet material, coated with an adhesive. Successive layers are cut out in the required shape and stacked to build up the part. Input materials can theoretically be paper, plastic, and even metal [4].
6. **Binder jetting:** This process enables deposition of powder material selectively with the application of a liquid adhesive.
7. **Direct energy deposition:** In direct energy deposition the powder metal and a laser beam are simultaneously pointed on a build plate where powder metal is melted and deposited.

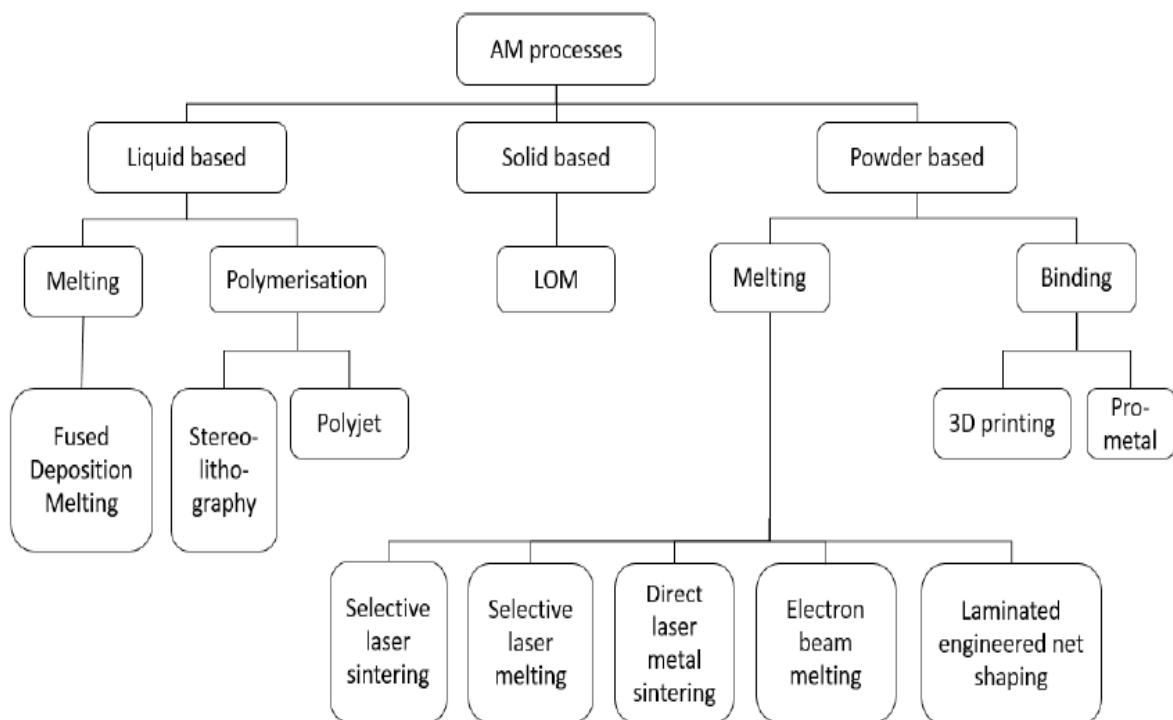


Figure 1 Various AM processes [5]

1.2.1. Process chain of AM

Additive manufacturing undergoes the following process chain to complete a 3D print:

- **CAD Design:** The first step is designing, in which a 3D model is prepared in any CAD based software
- **STL file creation:** STL (an abbreviation of "stereolithography") is the standard format used in all the additive manufacturing machines.

- **Parameters and Setup:** Before transferring the 3D design for printing, it is processed in a slicer software. Material selection, nozzle diameter and other parameters are selected. Similarly, layer height, infill density, printing temperature, build plate temperature and many other related parameters are defined. They come with default settings and can also be customised within the software. Finally, G-codes are generated.
- **Build:** G-codes can be sent to 3D printer for automatic printing. Although the process is automatic and follows the fed G-codes, however material and power should be monitored for the smooth operation.
- **Part removal:** After the printing is finished the part can be removed from build plate and the support structure (if used).

AM process usually produces finished products, however sometimes it requires postprocessing also.

1.2.2. Fused Deposition Modeling (FDM)

The process was initially developed by S. Scott Crump, Stratasys Inc., Eden Prairie, USA and protected by the patent US 5121329 A which expired in October 2009. FDM is one of the processes with a solid source material. In contrast to other additive processes, which also use solid source material like for example SLS (selective laser sintering) or 3DP (3D powder bed printing), the part is not built into a powder bed, but on an empty plate [3].

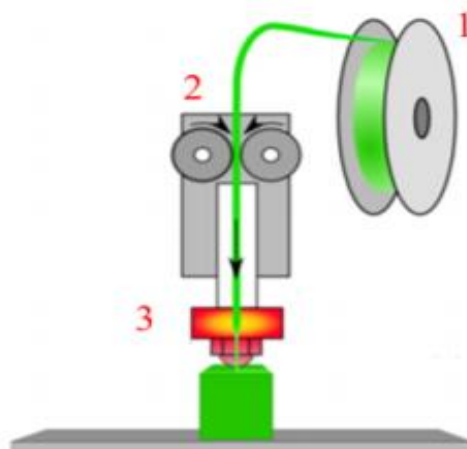


Figure 2 FDM process [8]

In the FDM process, a filament is extruded out of a heated nozzle and its molten thread is deposited on a heated build-plate. In our experimental work, a Creality Ender3 3D printer was

used in which the head moves in the X and Z directions according to the required geometry while the build-plate moves in Y direction. This machine uses a single nozzle for the deposition of molten material. One of the main benefits of this machine is its non-toxic, cheap, and odourless materials and come with various colours. The most common materials used for this process are ABS and PLA, however we have used PLA for its easier printability.

Currently, only thermoplastic filaments are used as feedstocks in FDM, including acrylonitrile butadiene styrene (ABS), polycarbonate (PC), polylactide (PLA), polyamide (PA), and the mixtures of any two of thermoplastics materials [1].

Materials	Characteristics
ABS	<ul style="list-style-type: none"> + Good strength + Good temperature resistance - More susceptible to warping
PLA	<ul style="list-style-type: none"> + Excellent visual quality + Easy to print with - Low impact strength
Nylon (PA)	<ul style="list-style-type: none"> + High strength + Excellent wear and chemical resistance - Low humidity resistance
PETG	<ul style="list-style-type: none"> + Food Safe* + Good strength + Easy to print with
TPU	<ul style="list-style-type: none"> + Very flexible - Difficult to print accurately
PEI	<ul style="list-style-type: none"> + Excellent strength to weight + Excellent fire and chemical resistance - High cost

Table 1 Different materials for FDM and their properties [7]

1.2.3. Benefits and Limitations of AM Technology

Ever since its emergence in 1980s, additive manufacturing has shown widespread popularity. Initially prototypes were produced for research purposes and gradually it gained success and got commercial value where finished products started to print. Although AM has been regarded as one of the great technologies in manufacturing sector and has great potential, yet it is young and along-with its numerous benefits it has certain limitations. Therefore, an overview of those pros and cons is presented for more insight.

1. Benefits

Free Complexity: It is cheaper to print a complex product than a simple one with same size when compared to traditional manufacturing processes. With additive manufacturing it can be printed faster and cheaper.

Reduced Lead Time: Manufacturing lead time is very important; in fact, a shorter lead time has competitive advantage. Manufacturing with AM technology reduces the lead time as engineers need to prepare the .STL file and print it. Similarly, they do not need to wait long, they can test the manufactured parts just after finishing.

Free Variety: This is probably one of the most significant benefits of AM. That is why AM technology is bringing about a revolution in mass customisation. If a part is needed to be modified, simply it is done in the CAD file and the modified version can be printed right-away.

Less Waste: The printed products are near net-shape, therefore, only the required materials need to complete the products, are utilised; as a result, no or very less scrap is produced.

Freedom in Manufacturing: There are less constraints in additive manufacturing than traditional one; almost anything that can be designed in CAD can be printed with a 3D printer.

No Assembly: Certain parts can directly be printed in the product itself, hence no or very fewer separate parts are printed for the same product. Therefore, time for assembly is saved, as a result, lead manufacturing time is saved.

Little-Skill Required: Apart from very specific and high-tech products with complicated parameters and design, additive manufacturing enables even elementary students to print their own products on a low-cost commercial 3D printer in their home.

2. Limitations

Although AM is regarded as one of the promising technologies with many benefits, some of which are listed above. There are also a few limitations and researchers are working to limit these cons in order to widespread its application.

Build Rate: Printing speed of AM processes is not very fast. Many 3D printers have a printing speed between 1 to 5 cubic inches per hour.

Lower Mechanical Properties: The layer-by-layer pattern of additive manufacturing may bring defects in the built part, as a result of which the mechanical properties are compromised.

Discontinuous Production: Additive manufacturing may prevent economies of scale because of the parts produced one at a time.

High Cost: Very high-quality additive manufacturing machines and the materials used for the purpose have high production costs.

Process	Description	Details	Advantages	Disadvantages	Applications
Selective Laser Sintering	Laser fusion in a powder bed	Layers: 0.06-0.15 mm Features: 0.3mm Surface: rough Print speed: fast	Strong Complex parts Large build volume Parts can be stacked in build volume Living hinges and snap features possible	Grainy surface finish	Electronics housing Mounts Custom consumer products Aerospace hardware
Stereo lithography	UV laser scanning vat polymerization	Layers: 0.06-0.15 mm Features: 0.1mm Surface: smooth Print speed: average	Fine detail Smooth surface finish	Weak parts Susceptible to sunlight and heat	Medical/dental products Electronics casings Investment casting patterns Art
Binder Jetting	Particle binding in a powder bed	Layers: 0.089-0.12 mm Features: 0.4mm Surface: rough Print speed: very fast	Multicolor prints Fast print speed	Very weak parts Rough surface finish	Full color prototypes and objects Figurines
Fused Deposition Modeling	Extruded layers of thermoplastic	Layers: 0.1-0.3 mm Surface: very rough finish Print speed: slow	High part strength Low cost	Poor surface finish Slow printing	Electronics housing Mounts Custom consumer products
Poly-jet	Jetted droplets of UV cross-linked polymer	Layers: 0.016-0.032 mm Features: 0.2mm	Fine detail High accuracy Multi-material capabilities	Low material strength Susceptible to sunlight and heat	Medical devices Complex and multi-material

Table 2 Advantages, disadvantages, and applications of various AM processes [6]

2. State-of-the-art

Additive manufacturing (AM) has gained commercial success in many applications, yet at present, intense research on AM is being carried out regarding geometry design, material design, computation tools, and manufacturing tools and process development [10]. Additive manufacturing has great potential for many reasons. This approach (AM) minimizes the number of equipment and the number of technological operations [14]. Not merely limited to prototypes, AM technologies are emerging in a way to replace the traditional manufacturing methodologies with the fact that they offer more flexibility for complex designs due the layer manufacturing approach. In fact, parts of significantly great complexity can be produced compared with traditional processes and this increased complexity generally does not have a significant effect on the cost of the process [17]. Moreover, additive manufacturing technologies provide new opportunities for the manufacturing of components with customisable geometries and mechanical properties [19]. In terms of successful applications of large-scale 3D printing or robotic fabrications, new experimental realizations emerge more and more often both from academia and industry, such as the contributions from IAAC, the autonomous construction rig from MIT or the 100 square meter house 3D printed in cement for the Milan Design Week 2018 (CLS Architetti), to name the very few [15]. Not only that, compared with conventional methods, AM can shorten the design-manufacturing cycle and thus reduces the production cost and increases the competitiveness.

FDM is the most widely used method among all the AM techniques for fabricating pure plastic parts with low cost, minimal wastage, and ease of material change [1]. It facilitates in printing complex products with acceptable strength. AM by material extrusion is the most cost-efficient and widely diffused technology for a wide variety of applications [2]. Indeed, in June 2013 there was news that National Aeronautics and Space Administration (NASA) plans to bring a 3D printer on board the International Space Station [4]. Recently the Italian Space Agency together with NASA installed two different FDM machines on the International Space Station limited to the production of PLA, ABS and PEI (ULTEM) samples [7].

Most of the work presented in the literature of Fused Deposition Modelling (FDM) are concerned with the mechanical properties of the parts produced by extrusion-based additive manufacturing technology. For instance, Wu et al. [9] presented a novel formulation for

generating porous structures firmly based on structural optimisation. This work revealed that the infill pattern and percentage significantly influence the printing process, as well as physical properties of the printed object. Obviously, a high-volume percentage usually leads to a material that can resist more the external loads, but thereby increasing the printing time for using additional material. To assist users in designing lightweight but mechanically strong prints, it is highly interesting to resort to structural analysis and optimization to find an optimal layout of the interior structure, which goes beyond the regular patterns [9]. There are numerous efforts to improve the properties of materials available for AM processes. These range from fill compositing technique using resins to improve the strength [11], multipolymer sandwich structures [13] (which basically increases the mass), carbon fiber-reinforced materials [1] and topology optimisation methods to solve a material distribution problem to generate an optimal topology [17]. In the work of Yu et al. [10] a hybrid topology optimization technique is presented in which the level set and DMO approaches are simultaneously applied to design and optimize the multi-patch FDM parts. With the proposed technique, the concurrent material domain optimization, material domain decomposition with distinguished raster directions, and multi raster angle optimization have been realized.

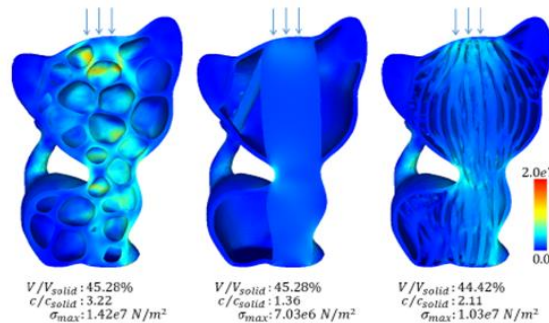


Figure 3 Honeycomb structure (left), structure (left), structure generated by topology optimisation (middle) and with local volume constraints (right) [9]

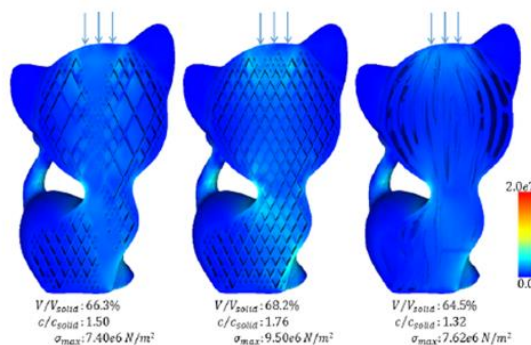


Figure 4 Self-supporting rhombic infill structure that are refined adaptively (left), and uniformly (middle) and structure generated by local volume constrained topology optimisation (right) [9]

The above pictures represent numerically optimised structures which resemble trabecular bone. Such optimised parts are lightweight and robust with less material used. The optimised interior of such structures uses best application of infill in additive manufacturing.

Similarly, T. Belter et al. [11] showed that the build orientation and extrusion path parameters all influence on overall part strength which shows the fibers oriented parallel to the direction of stress resulted in better strength as compared to those oriented perpendicular to the direction of stress in flexural test. Compared to the transverse direction, the material's tensile and compressible strengths are found to be stronger in the raster direction [10].

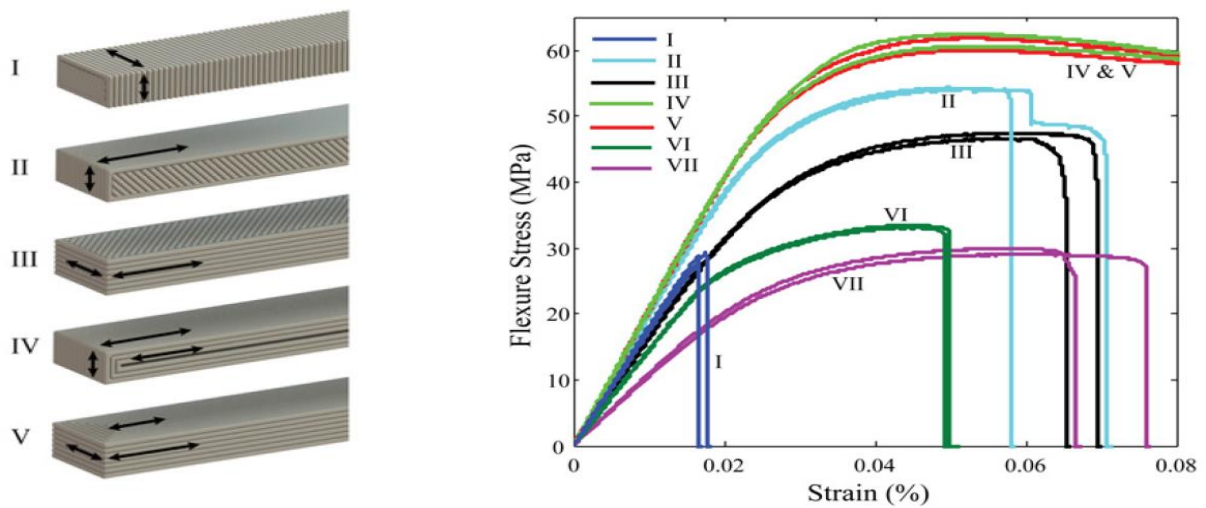


Figure 5 Influence of build orientation and extrusion path on the strength [11]

Moreover, sandwich structures made of different polymers combinations have been considered an excellent option to achieve various material properties for customized products, e.g. lightweight interior components in the automotive sector [13]. The author mentions the influence of shell, base thickness and infill density using PLA: optimising these process parameters can increase the part strength more than double of the original force that was required to fracture the same part and with a significant reduction of part mass as well to optimize the geometry of an FDM 3D printed part that can withstand higher loads.

The competitiveness of a product depends on its weight and cost of production. In order to achieve this objective, a solid product can be replaced by a shell with the same dimensions and geometry. The strength of the product can be ensured by forming the same material inside the shell. The volume fraction of this structure which is formed inside the shell varies from 0 to

100%. The strength of this structure is directly proportional to the volume fraction inside the shell. Terekhina et al. [14] studied the relationship between the volume fraction inside the shell (20–100% infill density) and the strength of the sample. Several groups of samples were made, for each of which a theoretical volume fraction of the filling structure was set: 20%, 40%, 60%, 80%, and 100%. As the degree of filling increases, the ability of the sample to plastic deformation increases (with shell).

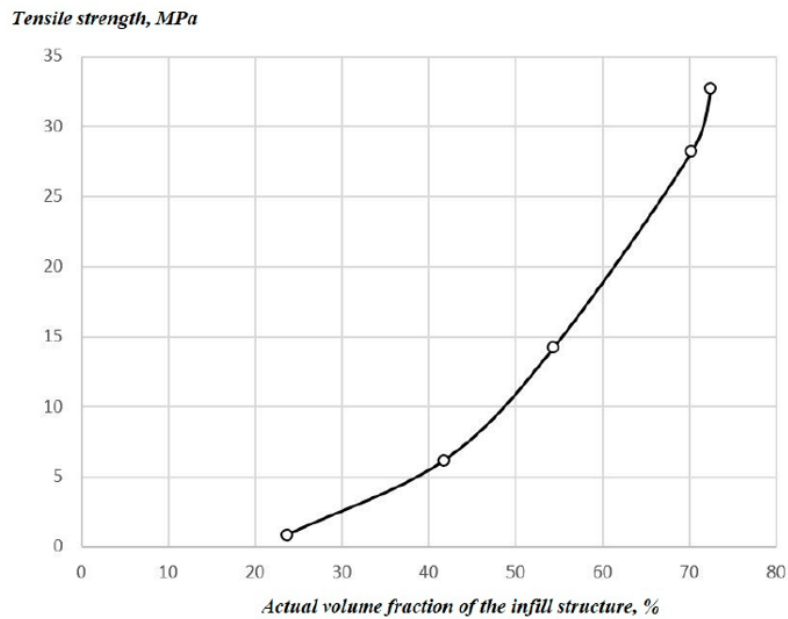


Figure 6 Dependence of tensile strength on the actual volume fraction of infill [14]

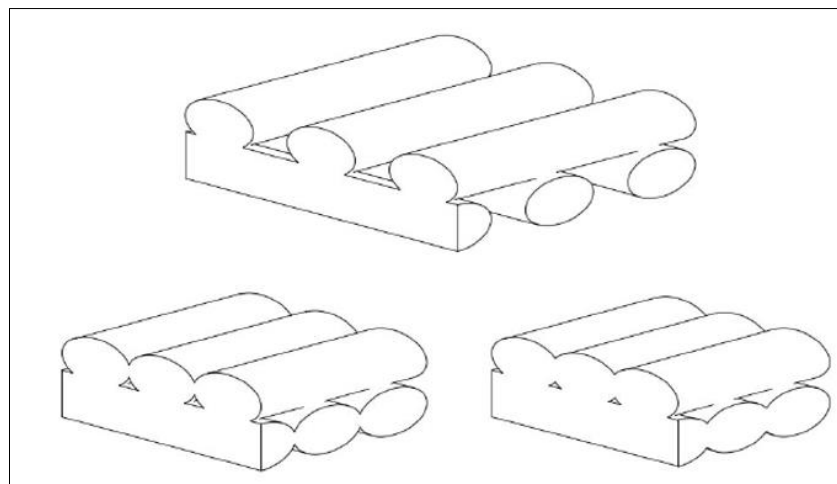


Figure 7 Tracks' interaction of different theoretical volume fractions of the infill structure: 40% (top), 80% (left), 100% (right) [14]

The obtained results show that with the increase of the volume fraction of the infill structure, the discrepancy between the preproduction (theoretical) and actual values is growing.

Increasing infill density from 20 to 60% leads to a negligible increase in relative strength [16] but carrying out a qualitative assessment of the results, it can be noted that after increasing the volume fraction of the infill structure above 60%, a significant increase in strength occurs [14] as indicated in fig 6. Another interesting result from the same researchers reveals that when setting a theoretical volume fraction of filling in the range of 20–40%, neighbouring tracks of the same layer do not touch each other. When the parameter is increased to 60% (which corresponds to the actual value of 54%), the parallel tracks contact (Figure 2.5), which leads to the formation of a continuous layer and increases the strength of the entire sample.

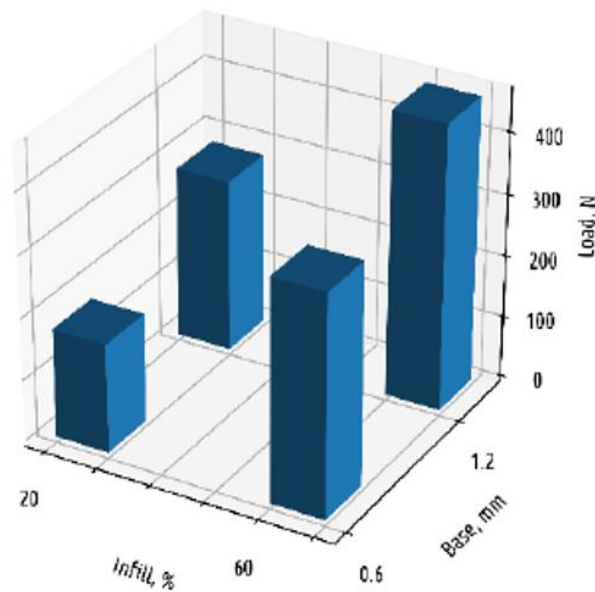


Figure 8 Fracture load depending on base thickness and infill density for samples with shell thickness of 1.2mm [16]

Infill density feature of additive manufacturing has been manipulated by many researchers. Clausen et al. [19] has recently introduced the so-called “coating approach” to topology optimisation. While standard topology optimisation approach produces solid structures, the coating approach results in structures with a solid shell and a porous interior. Higher the volume fraction, greater will be the strength [13] but it is expected that a good combination of topology and infill can lead to material properties comparable to that of a part with 100% mass.

Research have been carried out [8] to develop strategies to optimise the infill pattern of 3D printed parts based on their loading conditions. However, the area of topology optimisation of 3D printed parts and infill is still in its infancy. Thus, there exists great potential to expand this work and develop algorithms to optimise shapes and structures more complex than rectangular-

section beams. The conventional manufacturing techniques such as the subtractive (material removal processes) or formative processes (using molds) face several manufacturing constraints which need to be taken into account during the design phase otherwise many obstacles may arise during the actual processes such as tool access in case of machining or part removal from molds after casting. Consequently, the ultimate optimisation is limited and a trade-off between topology optimisation and ease of manufacturing has to be made. On contrary, AM enables the manufacture of the topology irrespective of the complexity and the cost of production does not usually increase with complexity [17]. Because of the layered manufacturing process, it is unnecessary to stick to the solid infill when designing mechanical components; instead, porous infill can be a good alternative as it demonstrates key advantages in high strength to relative low mass, good energy absorption, and high thermal and acoustic insulation compared to its solid counterpart [18].

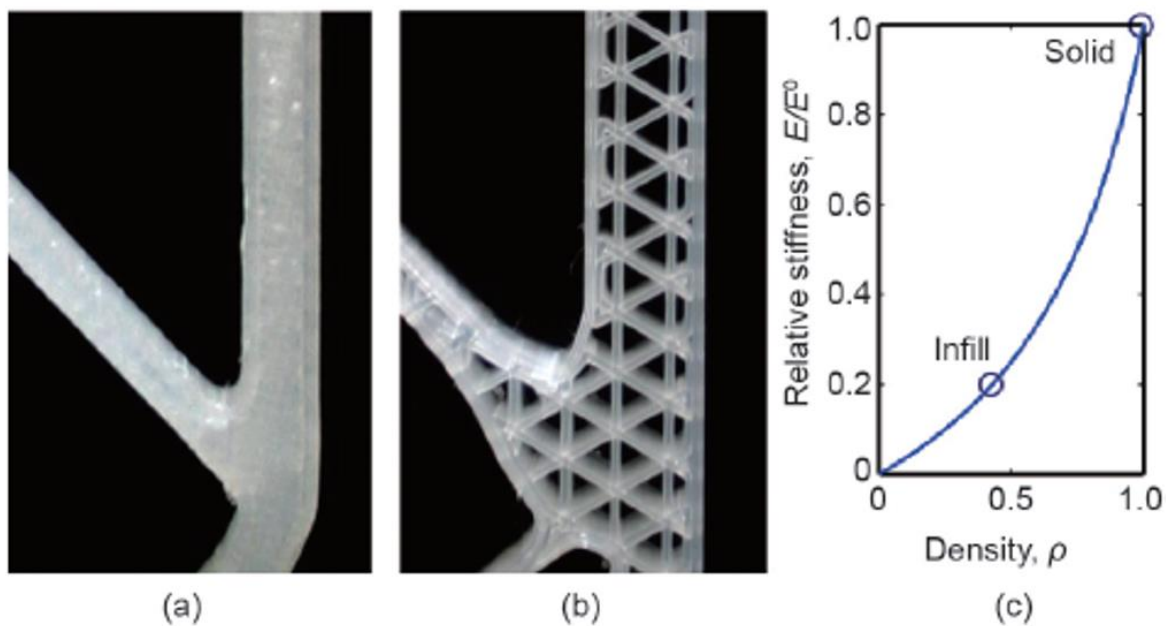


Figure 9 (a) Solid component (b) Porous component (c) Stiffness as a function of material density [18]

Not much literature is available that combines the cost with mechanical performance and weight in additive manufacturing. However, a couple of researchers have tried to investigate some of them. For example, Durgun et al. [25] analysed the production cost of FDM parts and concluded that the cost depends on the production time and material. The test results confirmed that the raster angle and orientation were important process parameters that affected the surface roughness, mechanical properties, and production costs.

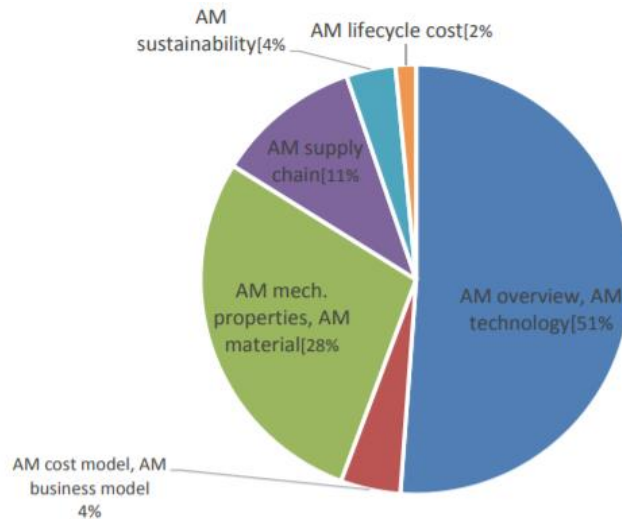


Figure 10 Mix of papers on additive manufacturing [27]

Moreover, for the FDM method, the build time and the amount of material can differ greatly for the same model because they depend on the orientation of the part. Time is reduced when less material is deposited and hence topology optimisation plays an important role for that. Apart from printing time and material consumed, there are other factors too which can contribute for the final product cost. Regardless of the technology in question (DMLS, EBM, LS, SLA and FDM), we can identify similar process phases that allow the definition of a single cost model valid for each of them. Some of involved factors are labour, machine, material, power source, warm-up time, build rate and energy consumption. By varying these factors, we obtain a different costs impact on the finished product [27].

Studies have been found on the influence of topology optimisation on the mechanical properties of printed parts [17][18][19]. Furthermore, several works have been reported to investigate the infill density, infill pattern as well as print direction on the mechanical properties [7][8][9][14][16]. However, there is a lack of published work on the combined effects of infill percentage and topology optimisation on overall part strength and manufacturing time and/or cost. This thesis work covers this gap, investigating the combined effects of topology optimisation and infill density on FDM printed parts using PLA, considering the cost and mechanical performance. Topologically optimised parts are printed in a shell with various percentage of mass reductions. The specimens included optimised solids, optimised porous and their combination with varying percentages of mass reduction are investigated.

3. Topology and infill

Topology optimization methods solve a material distribution problem to generate an optimal topology. It is usual for each finite element within the design domain to be defined as a design variable, allowing a variation in density or void-solid percentage. Often, the optimized topology is complex and due to manufacturing constraints commonly requires either simplification following the optimization process or constraining of the design space to only allow manufacturable designs. AM enables the manufacture of the topology irrespective of the complexity and the cost of production does not usually increase with complexity. In fact, sometimes the cost can decrease with increased complexity due to reduced support structure requirement. Processes where the part is produced by material removal can be described as subtractive processes and processes where the part is produced by a mold can be described as formative processes. These approaches have significant manufacturing constraints that must be considered during the design stage to ensure a feasible design. For example, the need for tool access in the case of machining or the need for part removal from a mold in the case of casting or molding. These constraints limit the physical realization of the optimal topology and a compromise must be made between optimality and ease of manufacture [17].

Manufacturing-oriented topology optimization has been extensively studied the past two decades particularly for the conventional manufacturing methods, for example, machining and injection moulding or casting [18]. Different from size and shape optimization, topology optimization as a freeform material distribution scheme, enables the creation, merging and splitting of the interior solids and voids during the structural evolution and therefore, a much larger design space can be explored, and superior structural performance can be expected compared with size and shape optimization. Because of the expanded design space, the gained topological design has often been criticized for being too organic, which poses challenges during the construction and post-editing of the associated CAD model. AM processes rely on layer-by-layer material deposition or solidification, which removes the geometric complexity restriction to a large extent. Besides, in AM, manufacturing efficiency and fabrication cost are not sensitive to geometric complexity. Therefore, AM can easily create freeform design from topology optimization, and many of the manufacturability related issues.

3.1. Topology optimisation

Topology optimization is an algorithm based on mathematical evaluation to make optimized material distribution in a part to be designed. Topology optimization (TO) is used at early stages of design to automatically reduce weight and material usage while satisfying constraints on performance [12]. Optimization of structures can be divided into size, shape, and topology optimization. Size optimization is commonly employed to find the optimal cross-sectional area of the beam in a frame or to find the optimal thickness of plate elements while satisfying design criteria. Shape optimization is characterized by a redefinition of the shape to obtain an optimal solution. This kind of optimization can reshape the material inside the domain keeping its topological properties. Topology optimization is the most general form of structural optimization. In discrete cases it is achieved by taking cross-sectional areas of bars as design variables, and hence allowing the resizing and the removal of bars in the frame. In continuum cases, topology optimization allows the best distribution of material inside the domain.



Figure 11 3D printed samples from topology optimisation [15]

3.1.1. Optimisation approach

Through topology optimization we can determine the overall configuration of elements in a design problem. Frequently, the results are used as inputs to subsequent size or shape optimization problems. Two main approaches have been developed: truss-based approach and density-based approach.

In the truss-based approach, a mesh of bars connecting nodes is defined in a predetermined volume, where the mesh can represent a complete graph (ground truss) or it is based on unit cells. Topology optimization proceeds to identify which bars are most important for the

problem, determines their size (especially area or radius) and removes bars so small that they have an insignificant contribution. Often result quality is a strong function of the starting mesh of bars. Results will resemble a lattice structure, with evident variations in bar radius.

The second approach is based on determining the appropriate material density in a set of elements called voxels which make up the spatial domain. This approach is the most common and famous and is employed in many commercial software packages. It became explicit through a process known as the SIMP (Solid Isotropic Material with Penalization) method. The starting geometry for the problem is a rectilinear block, which is composed of a set of voxels. Each voxel has a density value which is used as its design variable. A density value of 1 indicates that the material is fully dense, whereas a value of 0 indicates that no material is present. Intermediate values indicate which the material needs not be fully solid to support the local stress state in that voxel. Preferred solutions have voxels that are either fully dense or near 0 density, since typically partially dense materials are difficult to manufacture. Density values are employed to scale voxel stiffness values in the FEM models used during the optimization process.

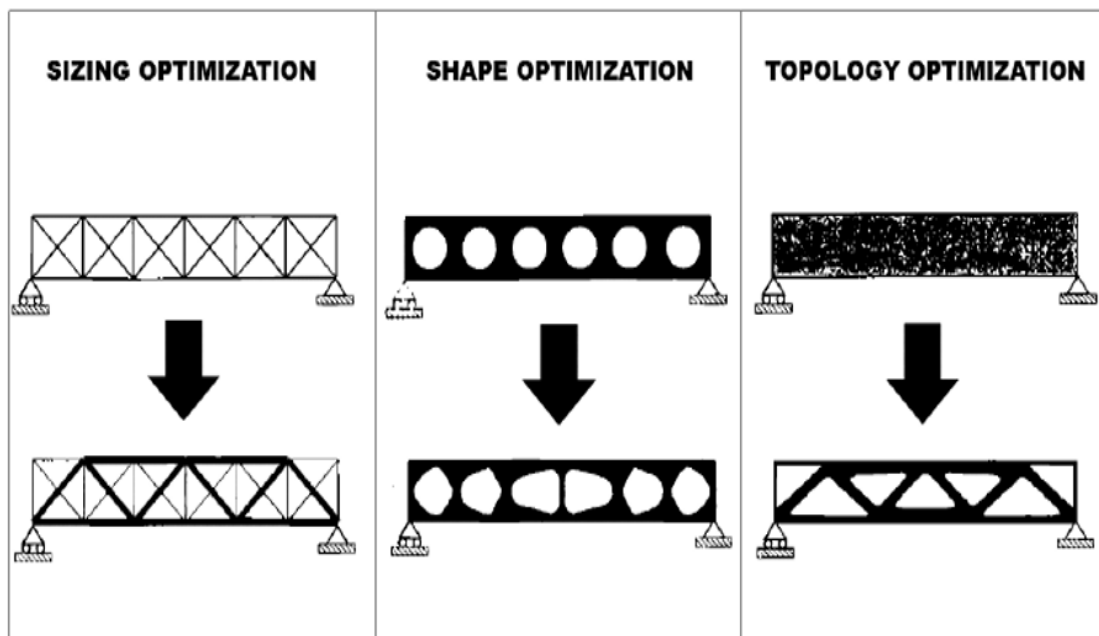


Figure 12 Size, shape, and continuum topology optimisation [12]

Topology optimisation is performed using two main methods elaborated below as:

Ground structure method:

The ground structure method [24] numerically approximates the optimal truss-like structure using a reduced finite number of truss members. The method “removes” unnecessary members from a highly interconnected truss (*ground structure*) while keeping the nodal locations fixed. The ground structure method has been refined, simplified, and optimized, resulting in an easy-to-use implementation for truss topology optimization in structured orthogonal domains.

Density-based topology optimisation:

Density-based topology optimization is a method that tries to answer, “What is the best distribution of material within a prescribed domain?”. It does so by discretizing the design domain and optimizing density variables associated to each element within the discretization.

Topology optimization is an iterative process. During the product design phase, the main queries to address are [12]:

1. What is the use of the product?
2. Which quantities are important for the product?
3. What is the goal I want to accomplish? And the constraints to be respected?
4. How do I optimize?

The traditional way of realizing the fourth step is via iterative-intuitive method:

- A specific design is suggested,
- Investigation phase (does the chosen design meet the imposed demands?),
- If demands are not satisfied, a new design must be suggested,
- The suggested new design is brought back to the second step.

An illustrative result:

As a result of the shape modification without going beyond the initial geometric boundaries is shown in Fig 13. It is possible to increase the relative strength.

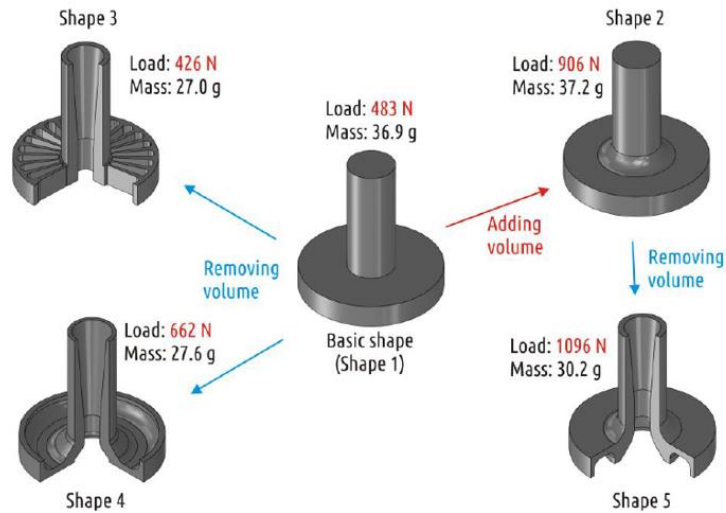


Figure 13 Shape optimisation path and results [15]

3.2. Infill density

In 3D printing, the structure that is printed inside an object is referred to as infill. It is generated in a designated pattern and percentage, which is governed by the selected thickness and scale. The infill settings along with the specific volume percentage are typically handled by the slicing software and may influence the material usage (weight), strength and print time. In general, a higher volume percentage leads to a print that is more resistant to external loads, while consuming more material and prolonging the print time. To assist users in designing lightweight but mechanically strong prints, it is highly interesting to resort to structural analysis and optimization to find an optimal layout of the interior structure, which goes beyond the regular patterns.

3D printing opens the door to optimizing the local infill density based on the actual stress fields and performance requirements, i.e., to manipulate infill wall thickness or infill feature size to achieve uniformly distributed stress. As this mapping can be fully automated and integrated in the computational design and digital fabrication process at no additional cost, there is no reason not to consider it [13].

3.3. Solid and porous structures

Because of the layered manufacturing process, it is unnecessary to stick to the solid infill when designing mechanical components; instead, porous infill can be a good alternative as it

demonstrates key advantages in high strength to relative low mass, good energy absorption, and high thermal and acoustic insulation compared to its solid counterpart. This decision is by default made by the slicer software e.g Ultimaker Cura (for G-code generation).

So far, however, topology optimization approaches have only been adapted to a minor degree to the new opportunities and the manufacturing constraints relevant for AM. Infill is an example of a unique feature of extrusion-based AM methods. It allows the creation of structures that are composed of a solid shell with a porous interior, as opposed to completely solid components.

The authors of this paper [18] have recently introduced the so-called coating approach to topology optimization. While standard topology optimization approaches produce solid structures, the coating approach results in structures with a solid shell and a porous interior, exactly as when using infill.

3.4. Effect on strength and stiffness

The coating approach offers no stiffness improvement. However, as shown in this study, it results in a strongly improved buckling load, which is an important element of structural stability. However, the cross-section changes from being fully solid to having a porous interior with a smaller homogenized stiffness. This means that the macroscopic axial stresses in the given bar are lower in the infill than in the corresponding fully solid bar by a factor depending on the skin thickness and infill density, while stresses in the solid shell are higher. While the structural stiffness decreases close to linearly (that is, compliance increases) when using lower infill percentages, the buckling load improves remarkably. This result is because lighter infill implies wider structural members, and that bending stiffness increases with a power of three [18] of the perpendicular distance from the centre axis.

By embedding a structured core to two stiff and thin outer layers, the mechanical properties of 3D-printed porous structures can be improved [21]. Design optimization toward high levels of stiffness and strength have the advantage of remaining components undamaged up to high stresses. However, if stresses are higher than the material strength, this type of optimized structure usually fails in a rather brittle and catastrophic way. On the contrary, optimization toward absorbed energy is more destruction tolerant but starts to damage earlier.

As shown in plots below, obtained from impact test [21], the force maximum increases independent of the infill structure with increasing infill density.

Similarly, to further improve the achievable levels of stiffness and energy absorption, the integration of topology and infill techniques were applied in this thesis.

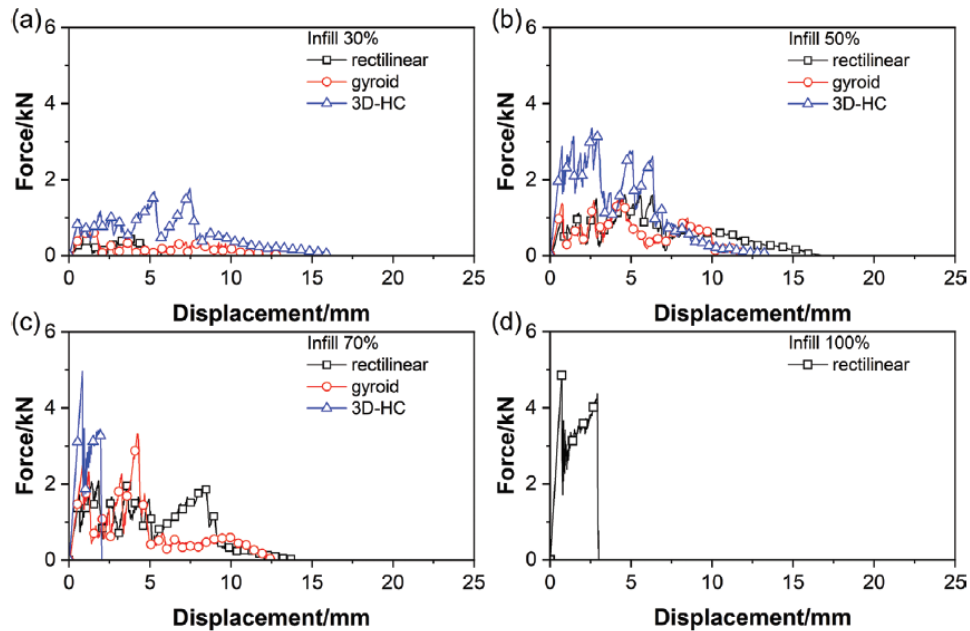


Figure 14 Maximum force as a function of infill structure and density [21]

3.5. Limitations and challenges

FDM is robust with respect to build scale and material. This, along with other advantages such as ease of use, portability, affordability, and safety make FDM very promising in producing functional parts in many applications [22]. The cost of AM parts increases significantly with material usage. Thus, optimizing designs can be crucial in saving material usage, build time, and post-process time.

However, there are certain challenges in TO for AM which need to be addressed before the two fields can be seamlessly integrated. Material anisotropy and weakness along build direction, especially in FDM, is an important consideration. This issue becomes more critical when the part is functional and has to satisfy strength-related constraint. There are mainly two types of anisotropy, namely 1) intrinsic e.g. composites and 2) process induced. Intrinsic anisotropy is often favourable since it can provide more freedom through intentionally creating

directional preference in behaviour. On the other hand, process-induced anisotropy is the result of process limitations and is often unfavourable.

3.6. Mass customisation

The term “mass customisation” was originally coined by Davis (1987) to describe the contradictory production strategy of realising mass production of customised objects; the principle was later developed by Pine (1993) [5].

MC attempts to bridge classic mass production and one-of-a-kind production. Figure 15 depicts the positioning of mass customisation approaches within the discussed matrix between mass production in the lower right-hand corner and production of different individual products in the top left-hand corner.

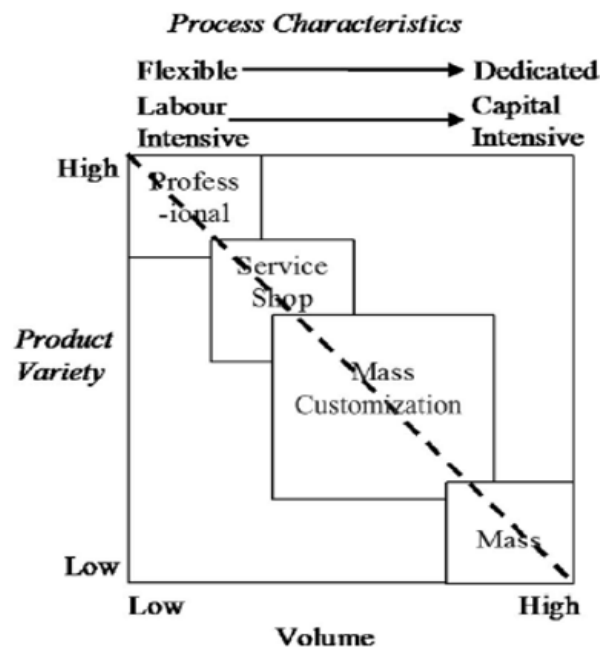


Figure 15 Product variety-volume matrix [5]

The term “customisation” implies that the customer has to be involved in the design process at some point in the product creation process. Similarly, the literature does not specifically define the level of production units required related to MC.

To make MC economically viable, suggests the degree of customisation be limited to the customer. Specifically, the principle of modularity in the product creation process is to combine standardised and customisable components. Modularity realises the feasibility of producing objects on a “mass” scale while variable elements ensure the “customisation” aspect.

With the introduction of AM, the realisation of Mass customisation has started to become more viable in both economic and technical perspective. The reduction of setup times that was previously taken by change of tools, fixtures and layouts is a promising feature of AM that has contributed towards MC. With the introduction of industry 4.0, customers can use the Rapid Manufacturing (RM) which enables them to customize their product, set priorities and order for manufacturing through internet [26].

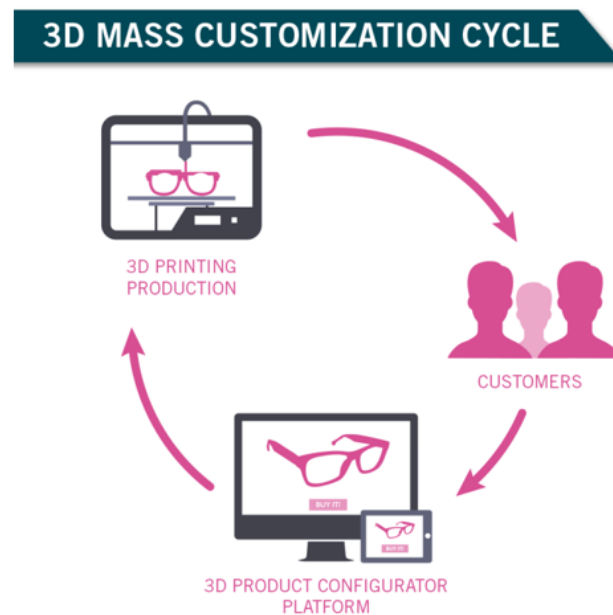


Figure 16 3D mass customisation cycle [26]

Consumer needs are now rapidly evolving with the advent of new technologies, materials and functionalities. Hence custom products are eventually going to be a priority for most customers in order to satisfy each individual's personal choice. One such field can be that of prosthetics where the part must satisfy and fit a certain requirement.

Of course, with customisation comes an increased price and the current engineering practice has been well developed. However, since the late 1980s, the success in customisation is now characterized by a good preliminary engineering design that makes this economically suitable and a technology of interest to multiple businesses [26].

4. Methodology

The aim of this research is to find the best possible combinations for mass reduction to produce lightweight products printed by Fused Deposition Modelling (FDM) using PLA as material under study. One of the main objectives is to retain the maximum possible strength and mechanical performance even after the mass is reduced to a certain degree using various mass reduction strategies such as topology optimisation, infill density and their integration. The literature review presents many applications of topology optimisation in traditional manufacturing but because of the shape complexities it comes-along many challenges and iterations are required in optimised parts as per manufacturing requirements. However, additive manufacturing incorporates maximum degree of topology because of the design freedom it offered without even extra cost of manufacturing. Considering the main objective of this research work, compression and tensile tests are conducted on optimised samples printed on a FDM machine (Crealty Ender3) to observe mass variation, load bearing capacity, stress concentration and other mechanical properties.

In the first step, topologically optimised parts were designed in a combination of different software in which the main objective was retaining the maximum stiffness, considering the load paths, as there can be various objectives of topology optimisation. A topology optimisation problem can be written in the general form of an optimisation problem as:

$$\text{minimise} \quad F = F(\mathbf{u}(\rho), \rho) = \int_{\Omega} f(\mathbf{u}(\rho), \rho) dV$$

The function $F(\mathbf{u}(\rho), \rho)$ represents the quantity that is being minimized for best performance. The most common objective function is compliance, where minimizing compliance leads to maximizing the stiffness of a structure. Topology study tries to get the stiffest structure possible given a certain amount of material removal.

While undergoing the design part for topology optimisation, goals and constraints have to be defined; in which you basically tell the software your design targets and terms of optimisation. In most of the optimisation software 3 types of optimisation are available:

- Best stiffness to weight ratio (Default)
- Minimise maximum displacement
- Minimise mass with displacement constraints

In order to retain the maximum stiffness, the first option is used and then the percentage mass reduction is selected.

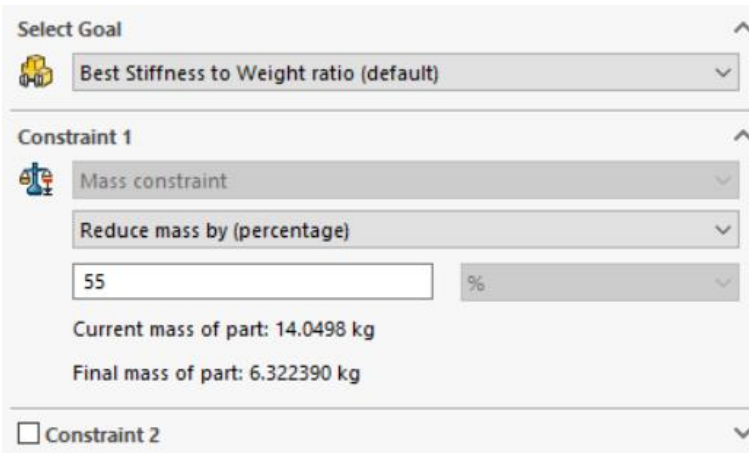


Figure 17 Goals and constraints panel in Solidworks 2018

The percentage mass reduction command reduces the original mass to a certain value; for example 6.3 kg, and computer takes this mass target and runs its iterations to get the stiffest part for this percent of mass retained and finally an optimised part is obtained as shown below.

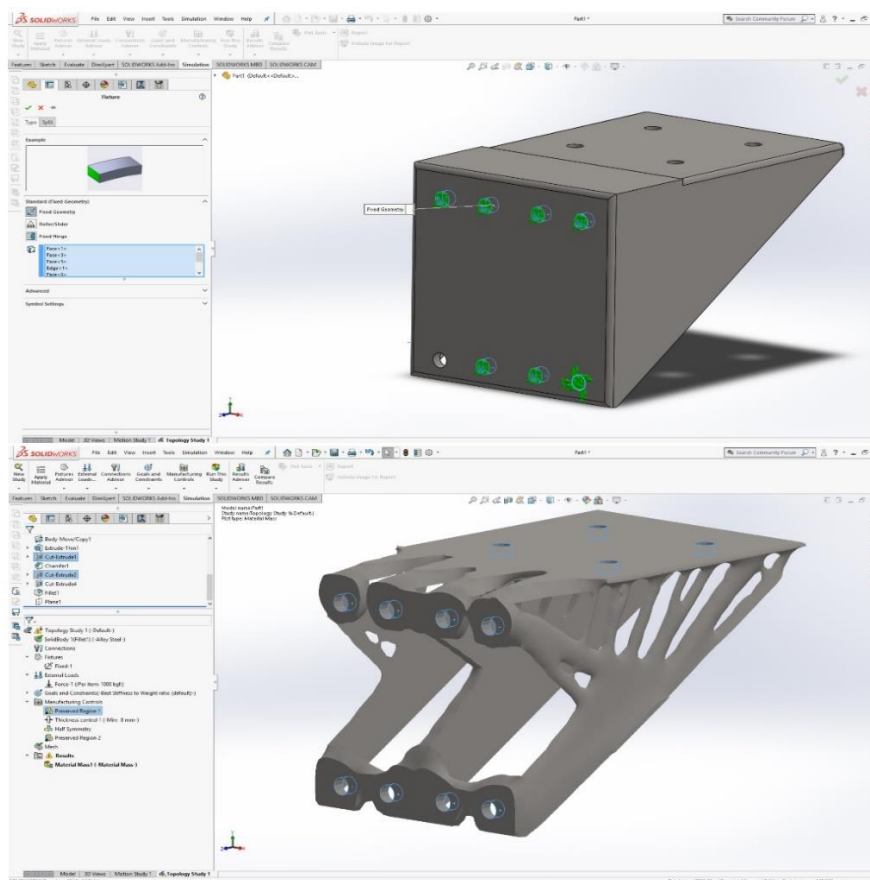


Figure 18 Topology optimisation of bracket in Solidworks 2018

In order to get the best optimisation and for G-codes generation for Creality Ender-3 FDM machine and deciding infill percentages and other settings a number of different software were used, they include:

- SolidThinking inspire
- ANSYS
- Ultimaker Cura

These are the software used in the desiging, analysing and for AM manufacturing stages. One of the main research concept in this thesis is topology optimisation which was achieved with the tools of these software, with varying percentages of mass as per the DOE of the thesis. These decisions are taken based on many objectives like maximum stiffness or maximum stress criterias. Various strategies are followed for topology optimisation based on the percentage of mass reduced, for instance a 80% topology means that 80% of the mass is retained from original part considering the maximum stiffness in that part as shown in the Figure 4.3.

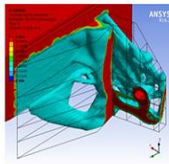
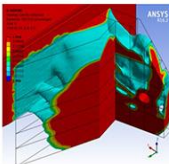
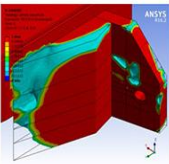

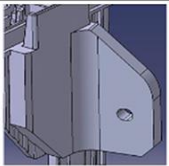

	CASE 1 Density 80%	CASE 2 Density 50%	CASE 3 Density 20%
Density Distribution			
Model			

Figure 19 Density distribution of topology optimisation

The methodology to meet the desired objectives of this thesis work requires various stages with the application of above mentioned software and printing the standard specimens with the present conditions and finally testing them for mechanical properties and analysing the obtained data to present the conclusions. For the better understanding of the methodology followed in this work, a detailed discussion is presented below.

The first step for this additive manufacturing based project was CAD modelling of desired compressive and tensile specimens in the above mentioned software.

After the modelling, a static structural analysis was performed on the compressive and tensile specimens on their yield strength in order to find the load path for topology. Similarly, the

design region and non-design regions were selected, the degree of topology optimisation like what percent of mass to be retained and topology criteria like maximum stiffness is selected. During the optimisation process the software runs numerous iterations to produce the best possible optimisation in the part with the selected degree and criteria of optimisation. Usually additive manufacturing can produce very complex optimised parts, yet the optimised design is validated and checked for its manufacturability. Moreover, the topologically optimised part is undergone static structural analysis to observe its behavior in different loading conditions and finally the design file is saved in STL format for 3D printing.

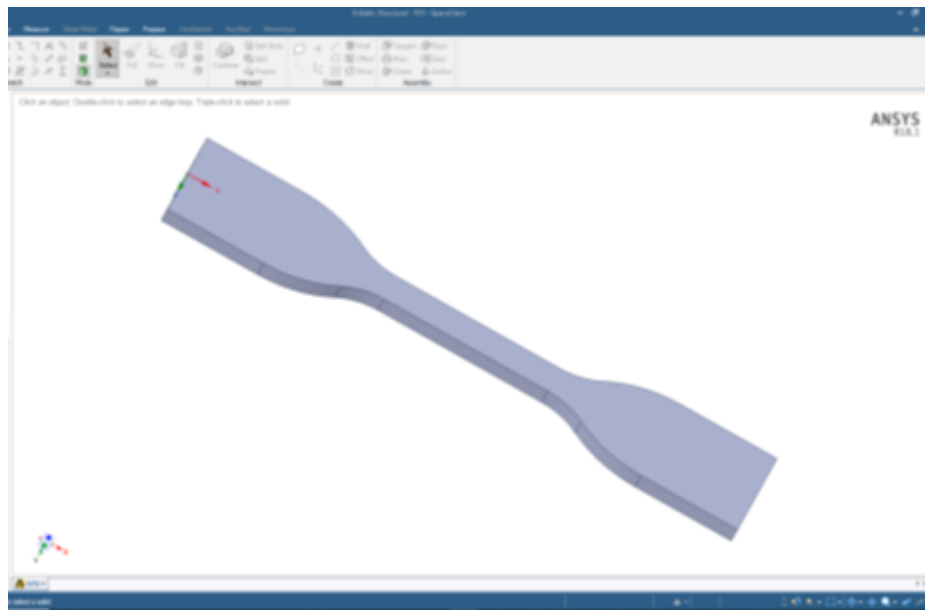


Figure 20 CAD model of tensile specimen

Now the samples are ready to be printed on a 3D printing machine. For this step, G-codes are generated for the samples to be printed. Ultimaker Cura (a slicing software) is used for slicing the STL files and generating G-codes. Moreover, the required infill percentage is selected for each sample as per the DOE of the research project along with other settings such as infill pattern, printing temperature, build plate temperature, nozzle diameter, layer height and other parameters. These process parameters are preselected and kept constant for each specimen except for the infill density as part of the DOE. The selection of such process parameters are specific to individual AM machines which can have their effects on the final printed parts such as the required surface finish, shape and porosity.

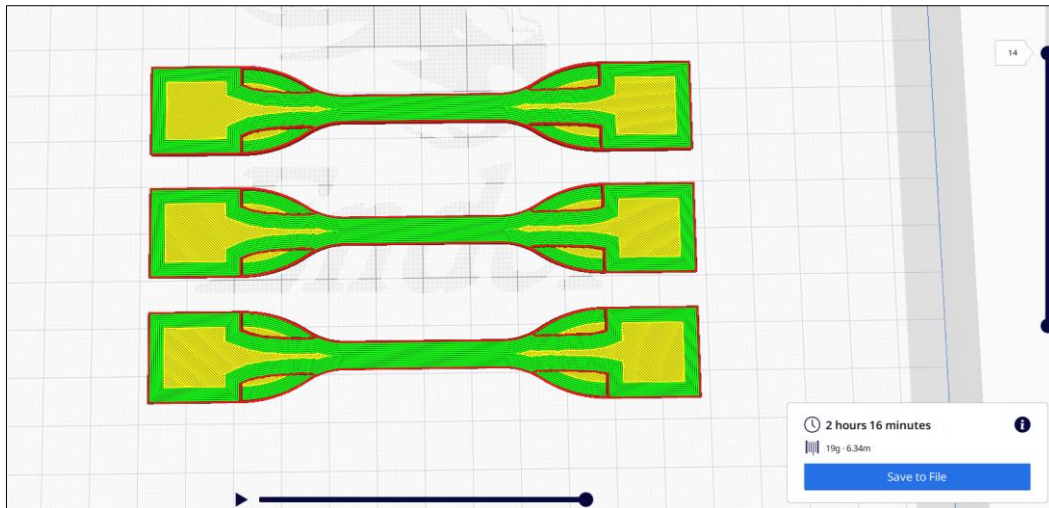


Figure 21 Sliced sample of 70% mass: 50% topology, 50% infill

The level of mass reduction in standard compression and tensile specimens for 5 levels are 100%, 85%, 70%, 50% and 30%. These different levels show the percentage mass retained. Mass reduction is done by topology optimization, infill density and a combination of both, using a proportion of 50:50, 33:67 and 66:34 for the combination of topology and infill. Therefore, 13 specimens for each compression and tensile with 5 different levels as mentioned above, taking 3 replicates for each strategy, 78 specimens are under study, as shown in table.

A	B	C	D	E	F	G
Part No	Mass% retained	By Topology	By Infill	Sample	STL file with Topology	Infill Density
1	50%	33%	67%	Compression	84%	67%
2	85%	33%	67%	Compression	95%	90%
3	50%	66%	34%	Compression	67%	83%
4	85%	66%	34%	Compression	90%	95%
5	30%	50%	50%	Compression	65%	65%
6	100%	50%	50%	Compression	100%	100%
7	70%	0%	100%	Compression	100%	70%
8	70%	100%	0%	Compression	70%	100%
9	70%	50%	50%	Compression	85%	85%
10	70%	50%	50%	Compression	85%	85%
11	70%	50%	50%	Compression	85%	85%
12	70%	50%	50%	Compression	85%	85%
13	70%	50%	50%	Compression	85%	85%
14	50%	33%	67%	Tensile	84%	67%
15	85%	33%	67%	Tensile	95%	90%
16	50%	66%	34%	Tensile	67%	83%
17	85%	66%	34%	Tensile	90%	95%
18	30%	50%	50%	Tensile	65%	65%
19	100%	50%	50%	Tensile	100%	100%
20	70%	0%	100%	Tensile	100%	70%
21	70%	100%	0%	Tensile	70%	100%
22	70%	50%	50%	Tensile	85%	85%
23	70%	50%	50%	Tensile	85%	85%
24	70%	50%	50%	Tensile	85%	85%
25	70%	50%	50%	Tensile	85%	85%
26	70%	50%	50%	Tensile	85%	85%

Table 3 Plan for mass reduction for each sample with relevant topology and infill %

Next step is experimental testing of the printed specimens on universal testing machines with proper parameters. The obtained data are analysed in minitab to find the best strategies and

conclusions are made accordingly. The details of such testing and analysis are detailed in the succeeding chapters.



Figure 22 3D printed Tensile and compression specimens

4.1. Tools for Topology Optimisation and Infill Density

Unless a part has been topologically optimised, usually it weighs more than it needs to be because of the redundant material used. As a result, the part becomes heavy, costly and higher shipping costs. Similarly, infill density can also be used where necessary; it can produce lightweight porous products for a variety of applications. The design freedom of additive manufacturing takes the best use of topology optimisation since AM can produce theoretically any optimised shape without an excess cost of manufacturing. Moreover, topology optimisation and infill density can be integrated to produce optimised parts with even less material consumption, thanks to the layered manner manufacturing.

One of the challenges in traditional manufacturing is mass customisation, where the entire process chain must be modified to meet the customised requirements of end users. On contrary, additive manufacturing provides such customised solutions because of its design freedom and flexible manufacturing solutions. Therefore, topology optimisation and infill density can combinedly provide even promising solutions for mass customisation. Many software and tools are used for topology optimisation and infill density settings; however, we have discussed the following software which have been used in this thesis work.

4.1.1. SolidThinking Inspire and ANSYS

These are probably among the most widely used software for topology optimisation and simulation in engineering sciences. Now a days, these software are also widely used for modelling of additive manufacturing components. ANSYS a mechanical finite element analysis software is used to simulate computer models of structures or machine components for analysing strength, toughness, elasticity, temperature distribution and many more. While SolidThinking Inspire is a powerful software that provides topology optimisation and rapid simulation solutions to engineers and researchers.

As per the pre-set objectives, standard compression and tensile specimens are created and exported to SolidThinking Inspire for topology optimisation. Following steps are followed for the purpose of topology optimisation:

- a) Material selection
- b) The design and non-design regions are selected in the samples. The tools used for this purpose include Combine, Partition and Cut etc
- c) The boundary conditions are defined i.e applying loads and constraints to characterise the tests (tensile and compression tests)
- d) The type of optimisation is selected such as topology optimisation or lattice structure.
- e) Selecting the optimisation level such as percentage mass reduction
- f) Finally defining the objective as maximize stiffness (or minimizing the compliance). Other options include minimising the natural frequency and displacement limitation.

After the topology optimisation is done as per the defined objectives and boundary conditions, the model was validated but because of the very high unacceptable stress-strain values results (in thousands of Mpa), it was not reliable to proceed with. Anyhow, this was validated when the model was analysed in ANSYS.

The following steps are carried out in ANSYS:

- a) Module selection: topology optimisation in our case
- b) Selecting the material

- c) Importing the model: stl. files are imported from SolidThinking Inspire and models were refined using tools such as wrapping and smooth to refine the surface
- d) From various available meshing options such as tetrahedral meshing, curvature sizing and proximity, mesh the model
- e) Boundary conditions defined
- f) Analysis

These are the preliminary steps before topology optimisation.

Objective definition: Maximize stiffness

- 1) Optimisation criteria: Mass reduction percentage
- 2) Design and non-design regions selection
- 3) Validate the optimised results, same as before

4.1.2. Ultimaker Cura

Once the parts were optimised with the above-mentioned procedures, they were saved in STL format and brought to Ultimaker Cura software for G-codes generation. The following steps are done:

- 1. Add the 3D printer from the list of available printers in the software; in this case Creality Ender3.
- 2. From custom settings, material and nozzle size are selected.
- 3. A profile can be selected from print settings with default parameters, or a customised profile can be made and saved with customized process parameters. In case of this thesis work a customised profile was made in which desired parameters with required values were selected. Some of such important parameters are reported in the figure 23.

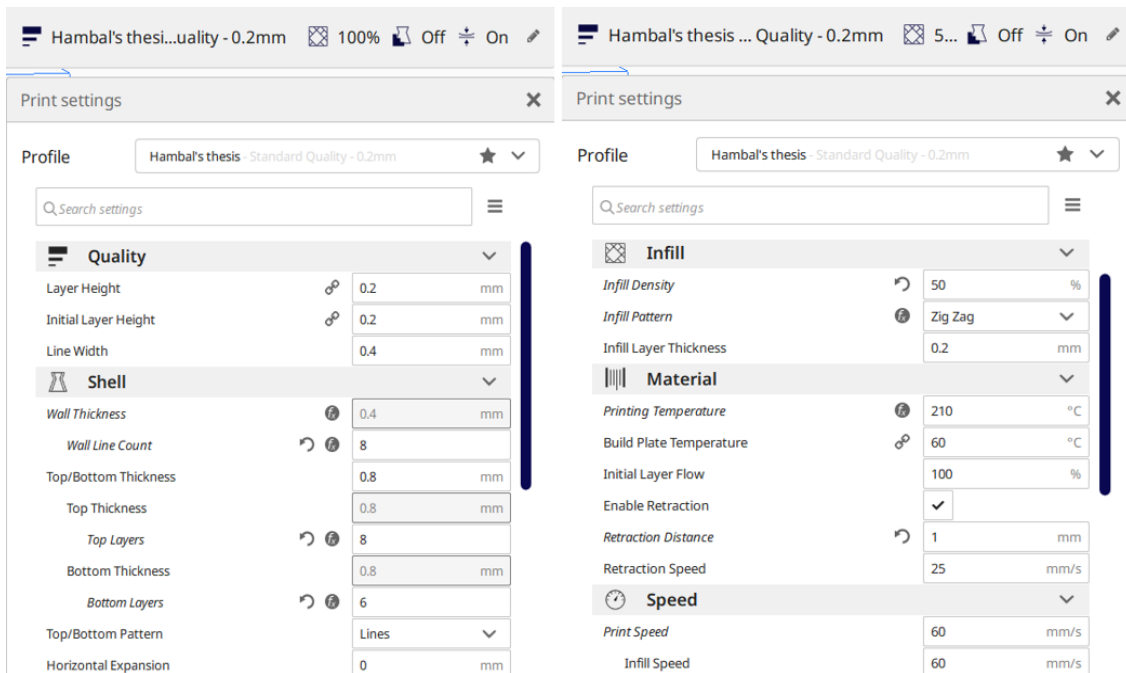


Figure 23 Important print parameters from Cura

4. The optimised parts were imported in STL. format. For each optimised part, the rest of the parameters were constant except the infill density was changed as per DOE.
5. Finally, the imported parts with desired parameters were sliced and G-codes were generated.

G-codes can either be saved and fed into 3D printer in a SD card or can directly be sent to 3D printer from Ultimaker Cura with the help of a data cable.

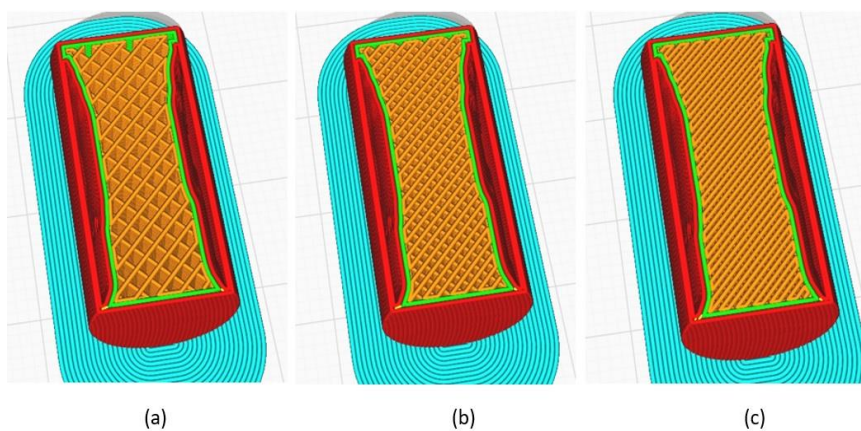


Figure 24 Topologically optimised parts with (a) 30%, (b) 50% and (c) 85% infill density

5. Experiments

The thesis starts from designing the specimens from software such as Solidthinking Inspire, fusion360 and ANSYS for basic design/dimensions and for various degrees of topology optimisation whose details have been presented in the previous chapters. Designed specimens were converted into .STL files and were taken to Cura for G-codes generation. Similarly, the G-codes were run on Creality Ender desktop 3D printer with pre-set parameters. FDM is an Extrusion-based Additive Manufacturing machine with very good surface finish, tolerance in affordable range. 78 specimens were printed with desktop FDM machine; 39 for each i.e Compression and Tensile tests.



Figure 25 FDM Machine



Figure 26 Tensile specimens optimised sections during printing

Extrusion-based additive manufacturing has the advantage of printing extreme level of topologically optimised parts which may not be printed with traditional manufacturing techniques. The design of these specimens is based on the so-called coating approach where the part is based on the internal structure which is optimised and printed with required infill density and then is covered in a shell. A similar case has been discussed in state-of-the-art.

The following steps are involved in such a design:

- a) The first layers consist of shell whose thickness and number of layers can also be defined from Cura
- b) Then the main body inside the shell is printed layer by layer and finally the outer shell skin is printed with subsequent layers
- c) For a fine surface finish, the printing speed and other parameters can be manipulated manually or from pre-defined settings.

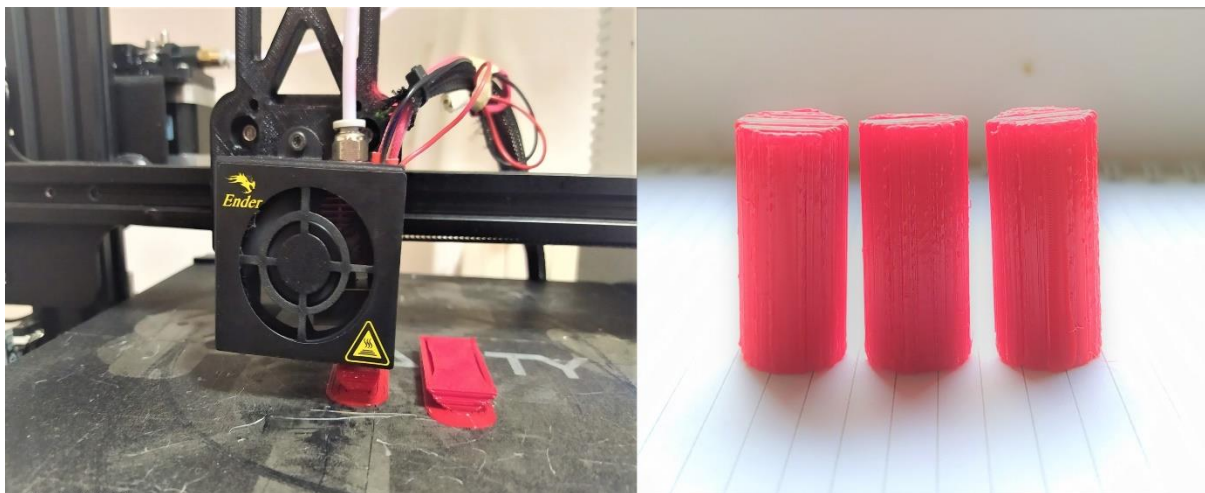


Figure 27 50% mass reduction, 66% by topology while 34% by infill density

5.1. Experimental Setup

Different mass reduction strategies (5 levels) are adopted with following combinations of topology and infill density percentages and 3 replicates are taken for each strategy and hence 39 specimens are printed for each test specimen i.e tensile and compression. Interesting results are expected with 70% mass, therefore, more combinations and replicates for this strategy are taken for iterative results to compare.

Experimental strategy for the research consists of Solid 100% infill, topology optimisation, infill density and topology + infill percentage with 15%, 30%, 50% and 70% mass reduction.

Strategies	Mass% retained	By Topology	By Infill
1	50%	33%	67%
2	85%	33%	67%
3	50%	66%	34%
4	85%	66%	34%
5	30%	50%	50%
6	100%	50%	50%
7	70%	0%	100%
8	70%	100%	0%
9	70%	50%	50%
10	70%	50%	50%
11	70%	50%	50%
12	70%	50%	50%
13	70%	50%	50%

Table 4 Different Mass reduction strategies

All the specimens were measured for weigh in controlled environment using Precisa. Moreover, the neck-width, thickness and length were measured for tensile specimens while the diameter and height for compression specimens were taken. Already the printing time for each specimen were recorded, such data can be very useful for measuring the cost coefficient.



Figure 28 Weight measurement

Finally, we were ready to test the 78 specimens for compression and tension. Since we have 3 replicates for each strategy, therefore, each replicate was assigned a different crosshead speed to observe the results. For this reason, 0.25, 2.5 and 25 mm/min crosshead speeds were used.

Sample No	Mass% retained	By Topology	By Infill	Test Type	Crosshead Speed (mm/min)	Weight (g)	D (mm)	h (mm)
1	50%	33%	67%	Compression	0.25	3.11	13	25.8
7	70%	0%	100%	Compression	0.25	3.27	13	25.9
14	50%	33%	67%	Compression	2.5	3.15	13.1	25.9
20	70%	0%	100%	Compression	2.5	3.2	13	25.9
27	50%	33%	67%	Compression	25	3.08	13.1	25.9
33	70%	0%	100%	Compression	25	3.27	13	25.8
Sample No	Mass% retained	By Topology	By Infill	Test Type	Crosshead Speed (mm/min)	Weight (g)	Thickness (mm)	Width (mm)
40	50%	33%	67%	Tensile	0.25	5.45	3.6	6.4
46	70%	0%	100%	Tensile	0.25	4.46	3.3	6.2
53	50%	33%	67%	Tensile	2.5	5.43	3.4	6.4
59	70%	0%	100%	Tensile	2.5	4.63	3.3	6
66	50%	33%	67%	Tensile	25	5.37	3.4	6.36
72	70%	0%	100%	Tensile	25	4.64	3.4	6

Table 5 Some random compression and tensile specimens with corresponding strategies, crosshead speeds and dimensions

5.2. Mechanical Testing

Mechanical testing of the printed specimens was performed using MTS Alliance RF/150 for compression and MTS Alliance RT/100 for tensile tests. The crosshead speed was set 0.25, 2.5 and 25 mm/min as per DOE for both compression and tensile specimens. The test results obtained are stress, strain, deformation, time of test, load and extensometer reading. From these results, Young's modulus, Yield strength, Ultimate tensile stress and strain at UTM can be calculated.

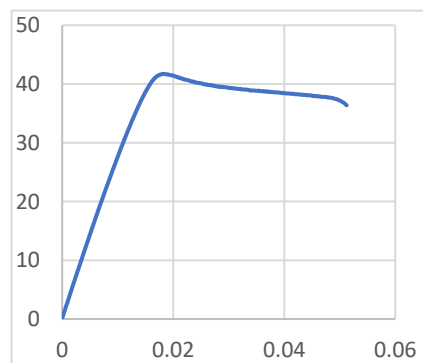


Figure 29 Stress-strain graph of 100% dense tensile specimen

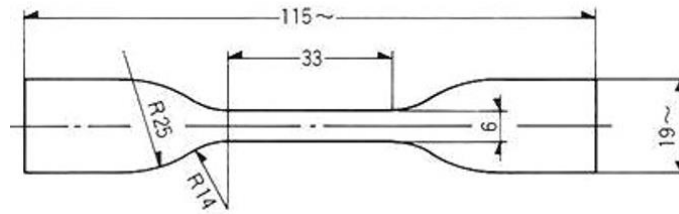


Figure 30 Standard for tensile test

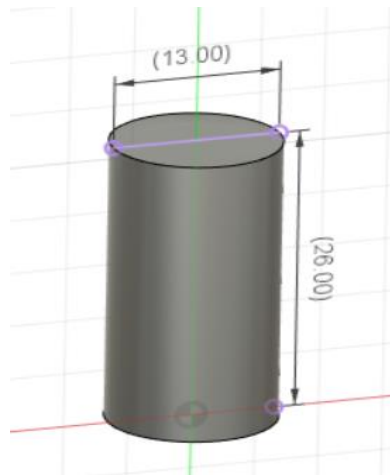


Figure 31 Standard for compression test



Figure 32 Compression and Tensile testing machines

From such experiments, stress, strain, maximum load, and deformation for each sample are used for analysis of results. Strain is measured from the standard strain gauge installed on the testing machine. Figure 33 of deformed specimens after experiment are used to point out the

stress concentration points and fracture mechanism. Topology optimisation is based on maximising stiffness on compression and tensile parts; therefore, density of material is increased at designed spaces. In tensile parts, the parts where they are clamped in non-design region.



Figure 33 Fracture points of different tensile samples

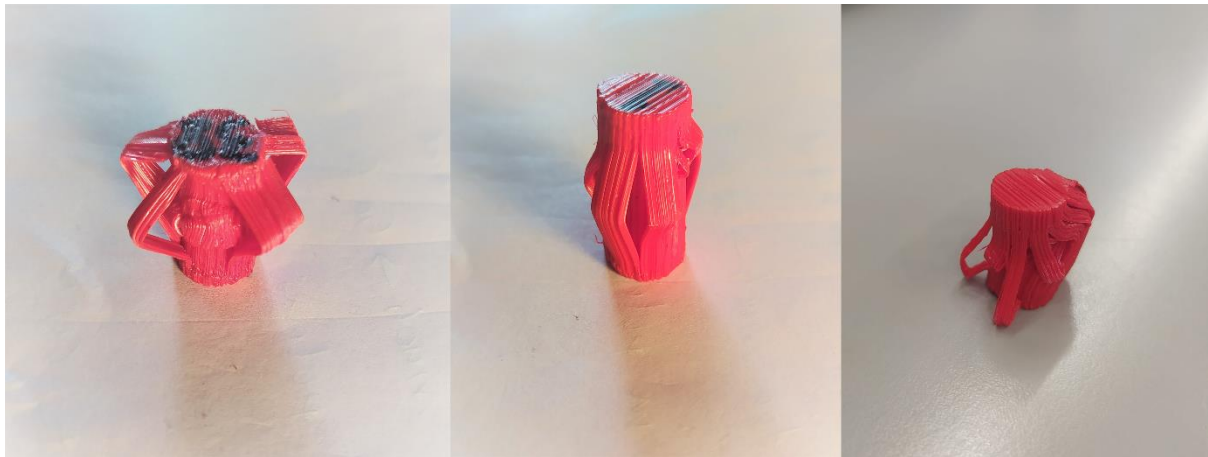


Figure 34 Fracture points of different compression samples

6. Results

6.1. Experimental Results

Experiments were conducted on 78 compression and tensile specimens with 5 levels of mass percentages and 5 levels of topology + infill combinations used for mass reduction which is tabulated in table 4 in previous chapter. Each combination was tested for a different crosshead speed to analyse the corresponding influence on the responses. Consequently, the effects of these factors are analysed on young's modulus, yield strength, ultimate tensile/compression strength, and cost coefficient. The experimental data obtained for young's modulus, yield strength, maximum tensile/compression strength and cost coefficient correspond to mass percentages of 50% and 85% with topology and infill ratios of 33:67, 66:34, respectively and mass percentages of 30% and 100% with topology and infill ratios of 50:50 each, while for 70% mass the topology and infill ratios are 0:100, 100:0 and 50:50, respectively. The same combinations are repeated for 3 crosshead speed of 0.25, 2.5 and 25 mm/min for both tensile and compression tests.

6.1.1. Compression Test

Data obtained from compression tests are analysed in Minitab as per above mentioned DOE using a General Linear Model analysis. We will observe the various outcomes from our analysis for each response resulting from the established factors.

Following shows the ANOVA tables for all the responses versus predefined factors.

Analysis of Variance

Source	DF	Adj SS	Adj MS	F-Value	P-Value
Mass% retained	4	7945935	1986484	3.31	0.031
By Topology	1	5063920	5063920	8.43	0.009
Crosshead Speed (mm/min)	2	15508	7754	0.01	0.987
By Topology*By Infill	1	1234267	1234267	2.06	0.167
By Topology*Crosshead Speed (mm/min)	2	268081	134041	0.22	0.802
Mass% retained*Crosshead Speed (mm/min)	8	3225339	403167	0.67	0.711
Error	20	12011483	600574		
Lack-of-Fit	8	6024201	753025	1.51	0.251
Pure Error	12	5987282	498940		
Total	38	29806240			

Model Summary

S	R-sq	R-sq(adj)	R-sq(pred)
774.967	59.70%	23.43%	*

Table 6 ANOVA of Young's Modulus for compression

With a confidence level of 95%, the ANOVA table reveals that Topology and Mass percentages are statistically significant on Young's modulus while crosshead speed is not. The model with corresponding R-square values is acceptable.

Analysis of Variance

Source	DF	Adj SS	Adj MS	F-Value	P-Value
Mass% retained	4	1588.06	397.016	5.83	0.003
By Topology	1	663.56	663.558	9.74	0.005
Crosshead Speed (mm/min)	2	104.48	52.242	0.77	0.478
By Topology*By Infill	1	207.46	207.459	3.04	0.096
By Topology*Crosshead Speed (mm/min)	2	4.81	2.403	0.04	0.965
Mass% retained*Crosshead Speed (mm/min)	8	146.47	18.309	0.27	0.969
Error	20	1363.12	68.156		
Lack-of-Fit	8	331.52	41.441	0.48	0.847
Pure Error	12	1031.60	85.967		
Total	38	4572.77			

Model Summary

S	R-sq	R-sq(adj)	R-sq(pred)
8.25568	70.19%	43.36%	*

Table 7 ANOVA of Yield Strength for compression

Similar conclusions can be presented for yield strength too. Except for crosshead, the mass percentage and topology optimisation levels are significant factors for yield strength.

Analysis of Variance

Source	DF	Adj SS	Adj MS	F-Value	P-Value
Mass% retained	4	1678.06	419.515	6.93	0.001
By Topology	1	763.55	763.549	12.62	0.002
Crosshead Speed (mm/min)	2	66.66	33.330	0.55	0.585
By Topology*By Infill	1	261.65	261.646	4.33	0.051
By Topology*Crosshead Speed (mm/min)	2	10.01	5.007	0.08	0.921
Mass% retained*Crosshead Speed (mm/min)	8	84.26	10.532	0.17	0.992
Error	20	1209.87	60.494		
Lack-of-Fit	8	186.27	23.284	0.27	0.963
Pure Error	12	1023.60	85.300		
Total	38	4545.44			

Model Summary

S	R-sq	R-sq(adj)	R-sq(pred)
7.77776	73.38%	49.43%	*

Table 8 ANOVA of Maximum Compression strength

Similarly, mass and topology are statistically significant for the case of Maximum compressive strength. In fact, mass percentage seems to be comparatively more considerable as compared to young's modulus and yield strength.

Moreover, the interaction between topology optimisation and infill percentage is very close to the level of significance i.e 5%, we cannot say anything for sure, however, we will observe that in the interaction plot if their interactions are significant.

Analysis of Variance

Source	DF	Adj SS	Adj MS	F-Value	P-Value
Mass% retained	4	2157.43	539.36	14.95	0.000
By Topology	1	1648.50	1648.50	45.70	0.000
Crosshead Speed (mm/min)	2	0.62	0.31	0.01	0.991
By Topology*By Infill	1	1125.11	1125.11	31.19	0.000
By Topology*Crosshead Speed (mm/min)	2	1.49	0.74	0.02	0.980
Mass% retained*Crosshead Speed (mm/min)	8	1.46	0.18	0.01	1.000
Error	20	721.38	36.07		
Lack-of-Fit	8	212.96	26.62	0.63	0.741
Pure Error	12	508.42	42.37		
Total	38	4929.06			

Model Summary

S	R-sq	R-sq(adj)	R-sq(pred)
6.00576	85.36%	72.19%	*

Table 9 ANOVA of cost-coefficient for compression

The ANOVA table for cost coefficient represents the significant factors i.e mass percentage and topology. In addition, the interaction between topology optimisation levels and infill density is also significant.

For further investigation, we can refer to main effect plots to see how the responses are affected with varying levels of factors.

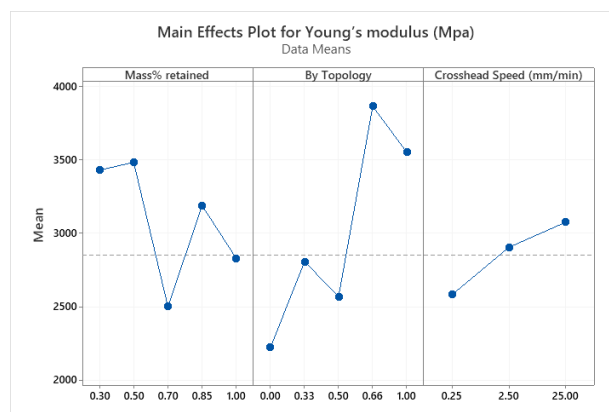


Figure 35 Main effects plot of E for compression

The main effects plot of Young’s modulus shows that a main effect exists for both mass percentage and topology optimisation, however their variation is not linear for increasing factor levels.

In this main effect plot, it appears that mass percentage of 50% is associated with the highest mean strength while 66% topology is associated with the highest mean strength. Crosshead, however, is linear but with least effect since it does not show significant variance from mean.

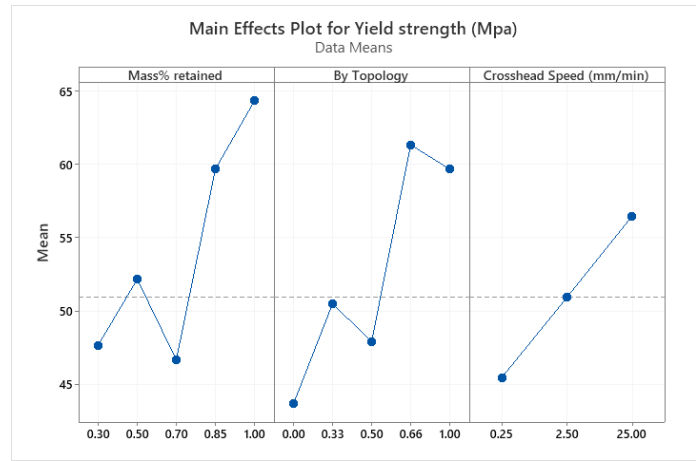


Figure 36 Main effects plot of YS for compression

100% mass and 66% topology are associated with the highest mean strength. For crosshead speed, the response mean is not same across 3 levels and it shows linear behaviour with highest mean strength at 25mm/min.

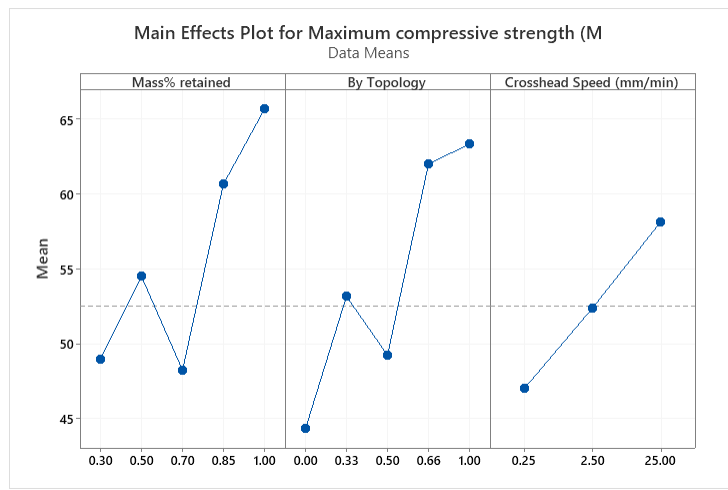


Figure 37 Main effects plot of maximum compression strength

Main effect is present with almost linear behaviour with highest mean strength of 100% mass, 100% topology and 25mm/min crosshead speed.

The main effects plot for cost below shows a linearly increasing effect of topology while no main effects are present for crosshead as seen in ANOVA table previously. For mass percentage we cannot conclude solely from main effects plot, but it represents its effects and also was significant from ANOVA table. If the interactions are significant, we cannot conclude merely from main effects plot. We can observe that in the interaction plot.

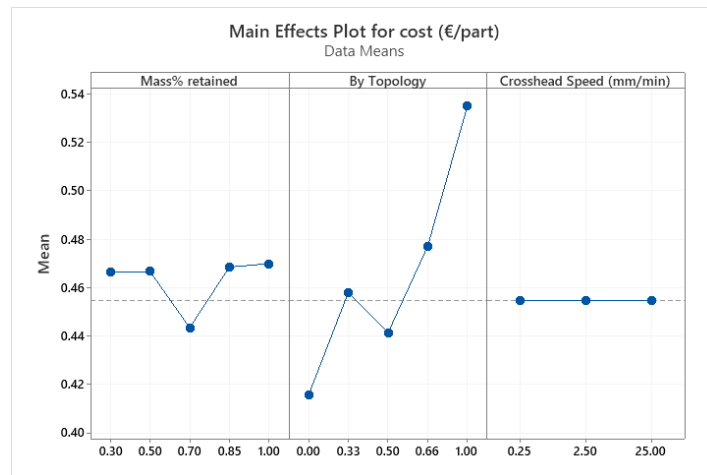


Figure 38 Main effects plot of cost-coefficient for compression

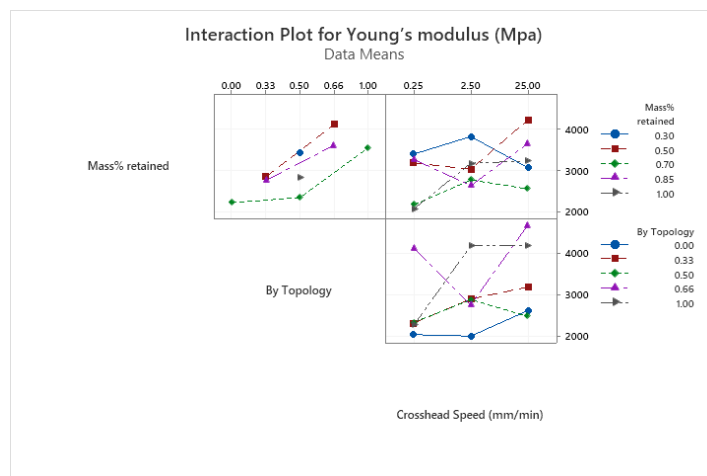


Figure 39 Interaction plot of E for compression

Interaction between mass*topology is less significant than interaction between mass*crosshead and topology*crosshead. The corresponding mean strength for Young's modulus can be seen for each combination, for example the highest mean strength for mass*topology is 50% mass and 66% topology.

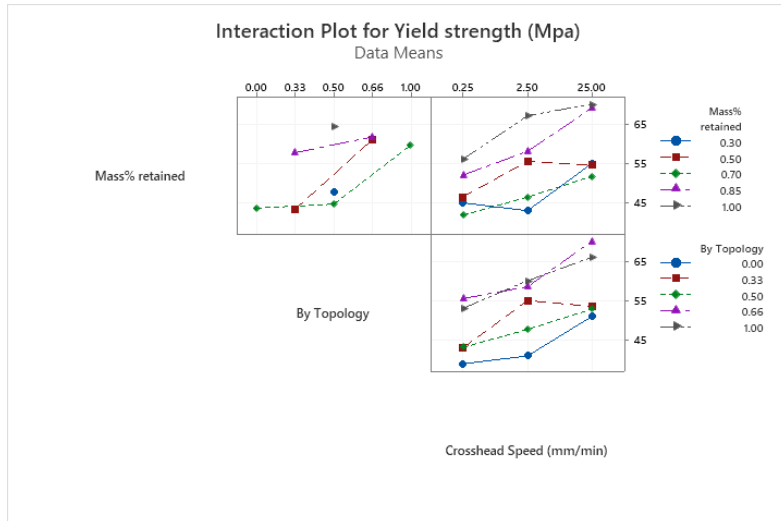


Figure 40 Interaction plot of YS for compression

Interaction among factors is significant for yield strength. It is noteworthy how the combination of different factors and levels effect the response, for example, at 50% mass with a topology contribution of 33% results in lowest mean strength while adopting 66% topology increases the mean strength to a level comparable with 85% mass with same level of topology optimisation.

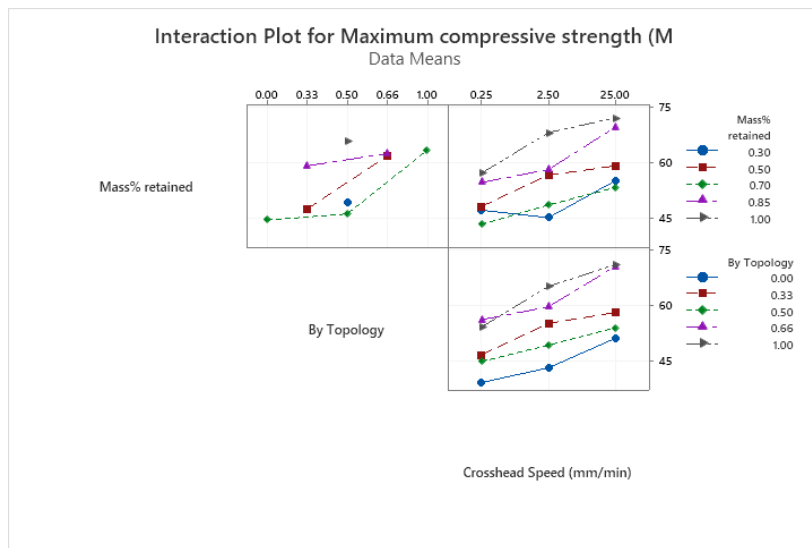


Figure 41 Main effects plot of maximum compression strength

Not very different from interaction plot of YS except with the fact that topology*crosshead shows a bit parallel lines for topology levels of 0 and 50 percent. But they may interact at some point, so we cannot say there is non-significant interaction.

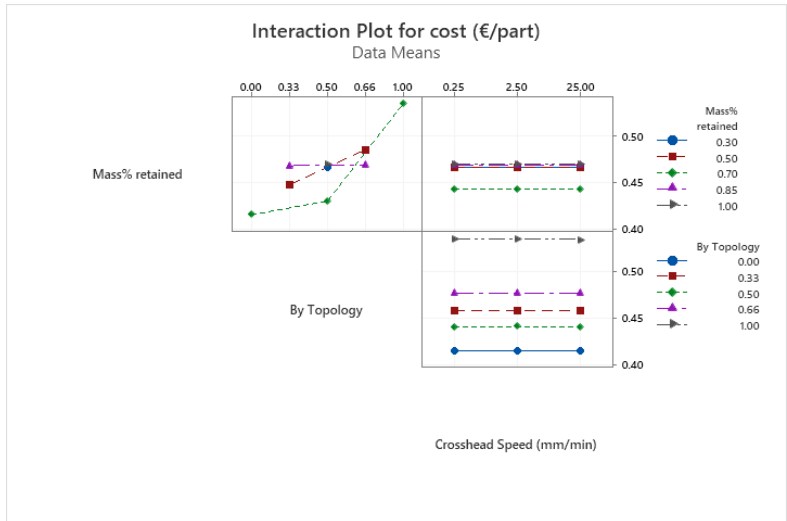


Figure 42 Main effects plot of cost-coefficient for compression

Interaction between mass*crosshead and topology*crosshead is not important since crosshead does not affect the cost of manufacturing, as seen in the graph. From this graph we can say that 50% mass with 66% topology and 34% infill density would be a good idea in terms of cost reduction while maintaining an acceptable strength as seen for the same combinations from previous plots. On the Contrary, 70% mass with 100% topology maximizes the cost.

Before concluding anything from the obtained data, it is advisable to check for the residual assumptions from normality test and scatter plot.

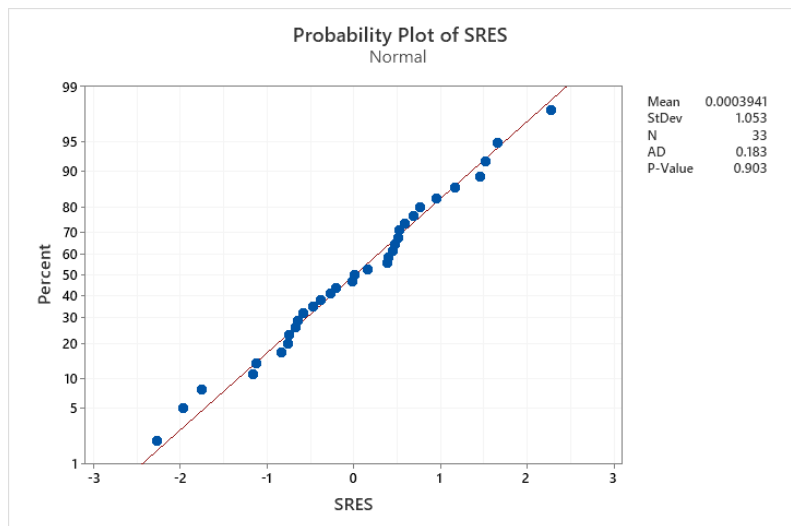


Figure 43 Probability plot of compression

The normality assumption cannot be rejected as the P-value is greater than 0.05.

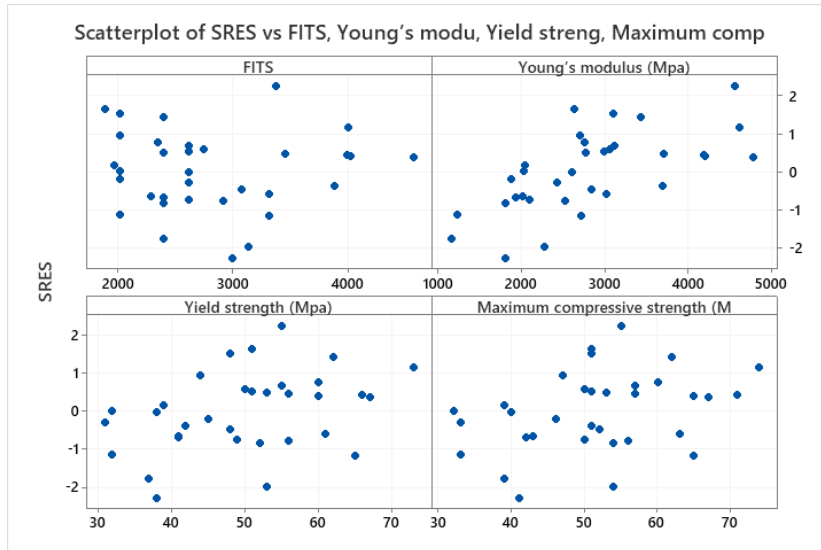


Figure 44 Scatter plot of SRES vs Fits, E, YS, Max compression strength

The SRES belong to the interval $[-3;3]$, thus we conclude that main effects are significant, and the interactions of some factors as seen in the interaction plots and ANOVA tables.

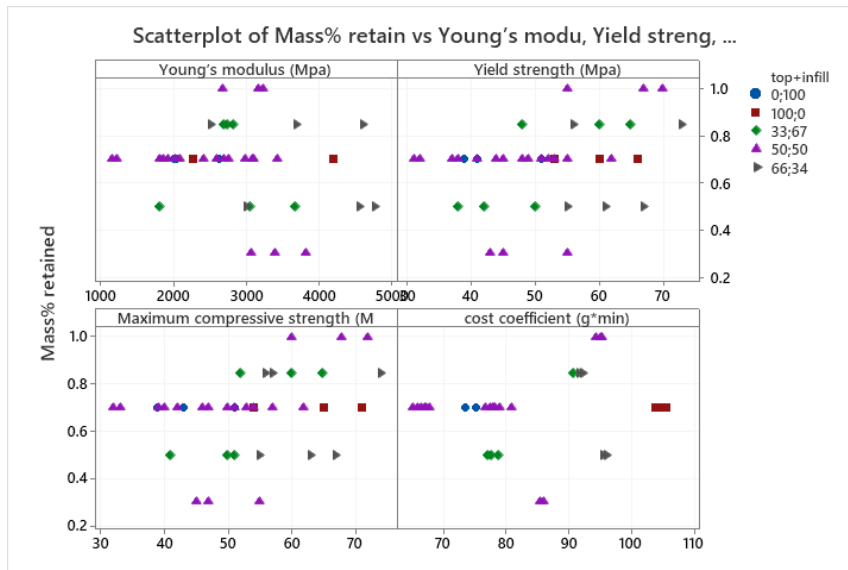


Figure 45 Scatterplot of Mass vs E, YS, cost-coefficient and maximum compression strength

The scatterplot shows the combination of topology and infill levels with mass percentage against each response.

6.1.2. Tensile Test

The same DOE with relevant factors and levels are analysed for tensile test data. The following outcomes are obtained.

Analysis of Variance

Source	DF	Adj SS	Adj MS	F-Value	P-Value
Mass% retained	4	570973	142743	7.36	0.001
By Topology	1	101581	101581	5.24	0.033
Crosshead Speed (mm/min)	2	2442	1221	0.06	0.939
By Topology*By Infill	1	678854	678854	35.02	0.000
By Topology*Crosshead Speed (mm/min)	2	10263	5132	0.26	0.770
Mass% retained*Crosshead Speed (mm/min)	8	173078	21635	1.12	0.394
Error	20	387681	19384		
Lack-of-Fit	8	295921	36990	4.84	0.008
Pure Error	12	91760	7647		
Total	38	1688744			

Model Summary

S	R-sq	R-sq(adj)	R-sq(pred)
139.227	77.04%	56.38%	*

Table 10 ANOVA of Young's Modulus for Tensile

From the ANOVA table we can conclude that mass percentage, topology optimisation and interaction between topology and infill percentage is significant for young's modulus.

Analysis of Variance

Source	DF	Adj SS	Adj MS	F-Value	P-Value
Mass% retained	4	357.54	89.385	13.39	0.000
By Topology	1	18.05	18.048	2.70	0.116
Crosshead Speed (mm/min)	2	135.87	67.937	10.18	0.001
By Topology*By Infill	1	380.88	380.876	57.05	0.000
By Topology*Crosshead Speed (mm/min)	2	9.17	4.585	0.69	0.515
Mass% retained*Crosshead Speed (mm/min)	8	26.68	3.335	0.50	0.842
Error	20	133.52	6.676		
Lack-of-Fit	8	93.92	11.739	3.56	0.024
Pure Error	12	39.60	3.300		
Total	38	1472.08			

Model Summary

S	R-sq	R-sq(adj)	R-sq(pred)
2.58376	90.93%	82.77%	*

Table 11 ANOVA of Yield Strength for Tensile

From the ANOVA table we can conclude that mass percentage and crosshead speed are significant factors, but topology is not significant for Yield Strength. However, the interaction

of topology and infill is significant. We can further verify such interactions between various factors in the interaction plots.

Analysis of Variance

Source	DF	Adj SS	Adj MS	F-Value	P-Value
Mass% retained	4	414.83	103.707	18.72	0.000
By Topology	1	20.71	20.712	3.74	0.067
Crosshead Speed (mm/min)	2	110.72	55.362	9.99	0.001
By Topology*By Infill	1	433.64	433.642	78.27	0.000
By Topology*Crosshead Speed (mm/min)	2	4.28	2.141	0.39	0.684
Mass% retained*Crosshead Speed (mm/min)	8	31.20	3.900	0.70	0.685
Error	20	110.81	5.540		
Lack-of-Fit	8	88.81	11.101	6.06	0.003
Pure Error	12	22.00	1.833		
Total	38	1481.90			

Model Summary

S	R-sq	R-sq(adj)	R-sq(pred)
2.35381	92.52%	85.79%	*

Table 12 ANOVA of Maximum Tensile Strength

Similar conclusions can be given for maximum tensile strength as seen in case of yield strength.

Analysis of Variance

Source	DF	Adj SS	Adj MS	F-Value	P-Value
Mass% retained	4	2572.81	643.203	8.25	0.000
By Topology	1	229.09	229.086	2.94	0.102
Crosshead Speed (mm/min)	2	3.50	1.752	0.02	0.978
By Topology*By Infill	1	458.14	458.142	5.88	0.025
By Topology*Crosshead Speed (mm/min)	2	20.45	10.225	0.13	0.878
Mass% retained*Crosshead Speed (mm/min)	8	89.74	11.218	0.14	0.996
Error	20	1559.13	77.956		
Lack-of-Fit	8	754.00	94.250	1.40	0.287
Pure Error	12	805.13	67.094		
Total	38	5612.12			

Model Summary

S	R-sq	R-sq(adj)	R-sq(pred)
8.82929	72.22%	47.22%	*

Table 13 ANOVA of cost-coefficient for Tensile

Amount of mass and interaction between topology and infill is significant for cost coefficient.

After going through ANOVA tables for each factor, we are interested to see the main effects of different factors for each response corresponding to various predefined levels.

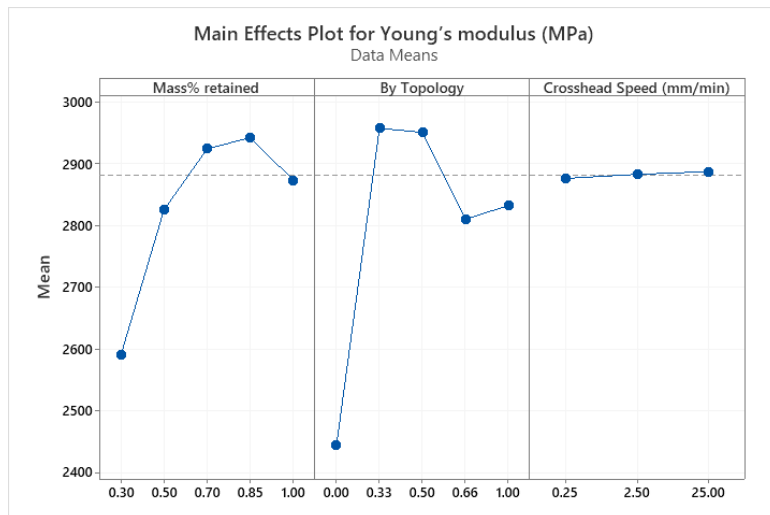


Figure 46 Main effects plot of E for Tensile

For crosshead speed, each level affects the response in the same way (nearly parallel with mean) and hence no main effects. Differently from ANOVA table, mass and topology has main effects for Young's modulus. Moreover, 85% mass and 33% topology represent main effects. But it is noteworthy that we are not considering the interactions here, maybe their interactions are significant and hence they can outline a clearer picture, we can see that in the interaction plot.

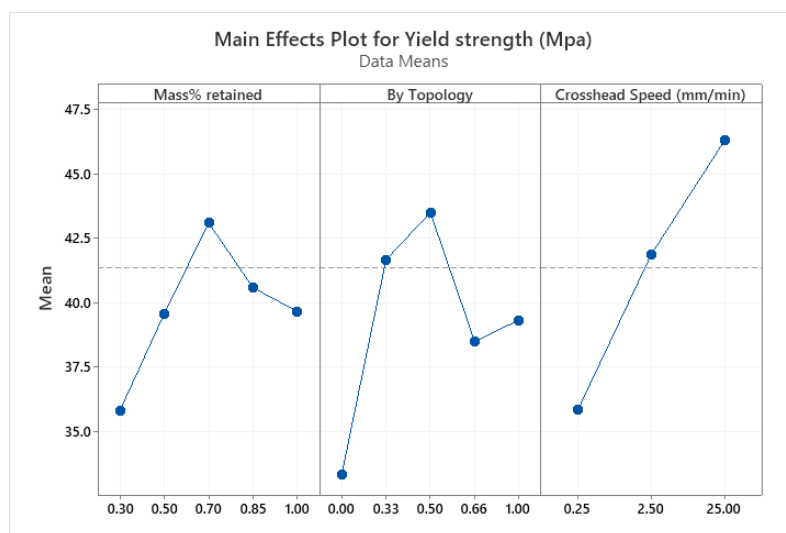


Figure 47 Main effects plot of Yield Strength for Tensile

Main effects are found for all factors and interestingly the crosshead speed shows a linear increasing pattern among 3 levels.

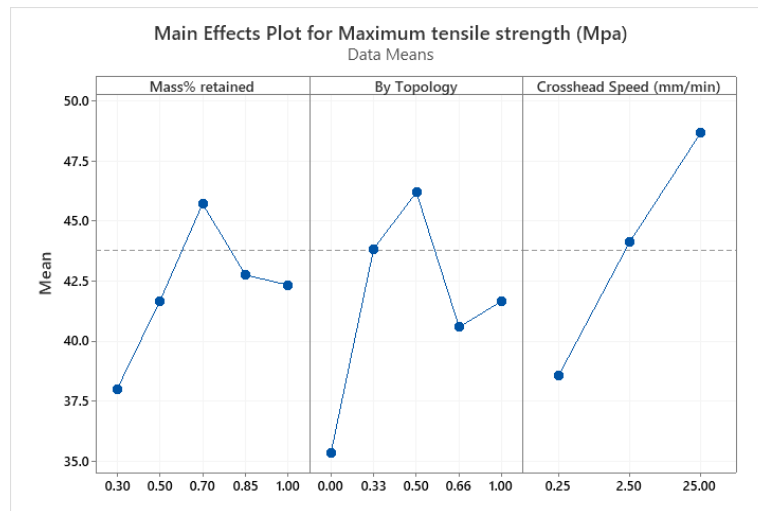


Figure 48 Main effects plot of Maximum tensile strength

Main effects plot for maximum tensile strength follows a similar pattern as seen in case of yield strength.



Figure 49 Main effects plot of cost-coefficient for Tensile

Like always, crosshead speed does not have main effects on cost while mass and topology do i.e 100% mass and 33% topology correspond to maximum cost.

Main effects plot alone cannot be used for concluding remarks; interactions between factors and corresponding levels can reveal interesting facts.

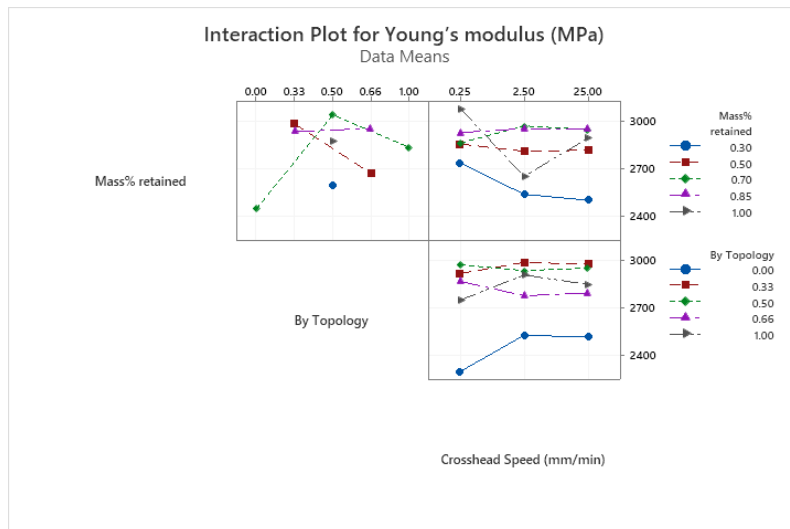


Figure 50 Interaction plot of E for Tensile

The interactions are significant, and it is interesting to see how these factors with relevant levels are interacting. Here we can observe a couple of combinations of mass percentage and topology optimisation levels which are competitive with the degree of closeness corresponding to Young's modulus such as 70% mass with 50:50 [topology: infill], 50% mass with 33:67 [topology: infill], and 85% mass with either 66:34 or 33:67 [topology: infill] combinations. The optimal levels can be chosen based on a techno-economic criterion based on the Young's modulus and mass consumed (i.e., cost).

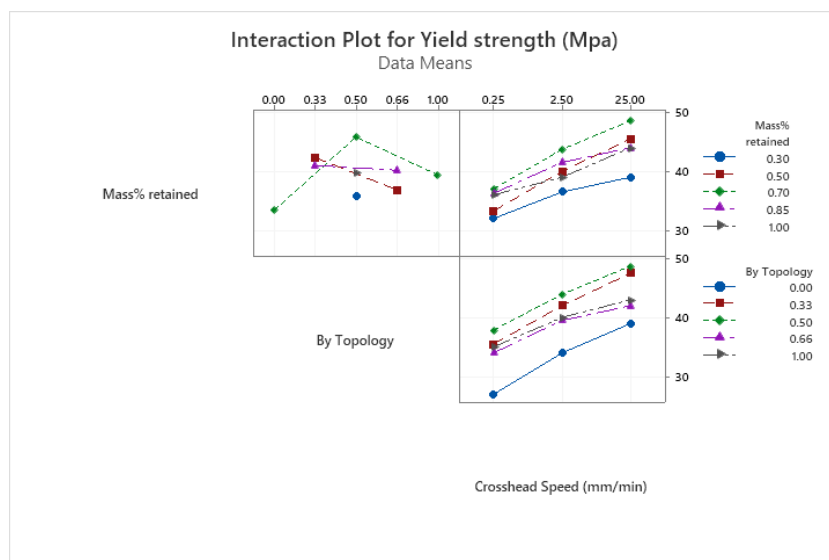


Figure 51 Interaction plot of Yield Strength for Tensile

Mass and topology have the most significant interactions for yield strength, for which 70% mass with 50:50 [topology: infill] is most important.

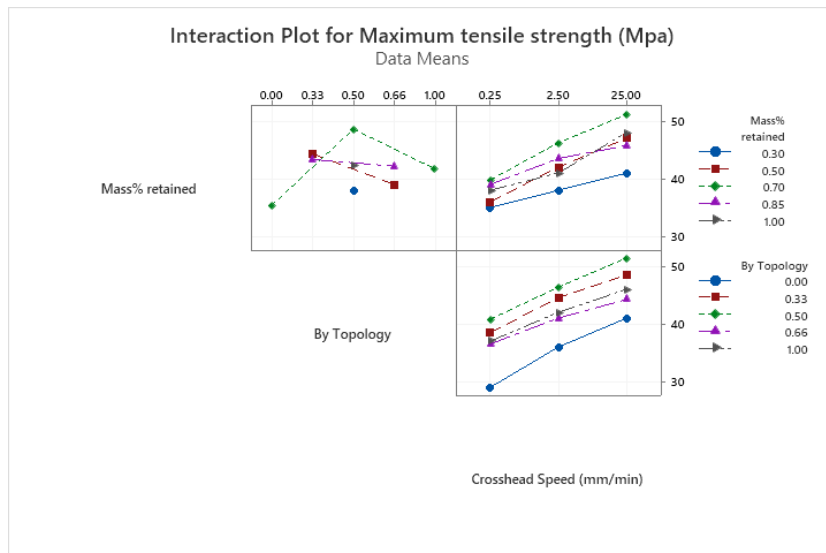


Figure 52 Interaction plot of Maximum Tensile Strength

Similar conclusions can be passed for maximum tensile strength as seen for the case of yield strength.

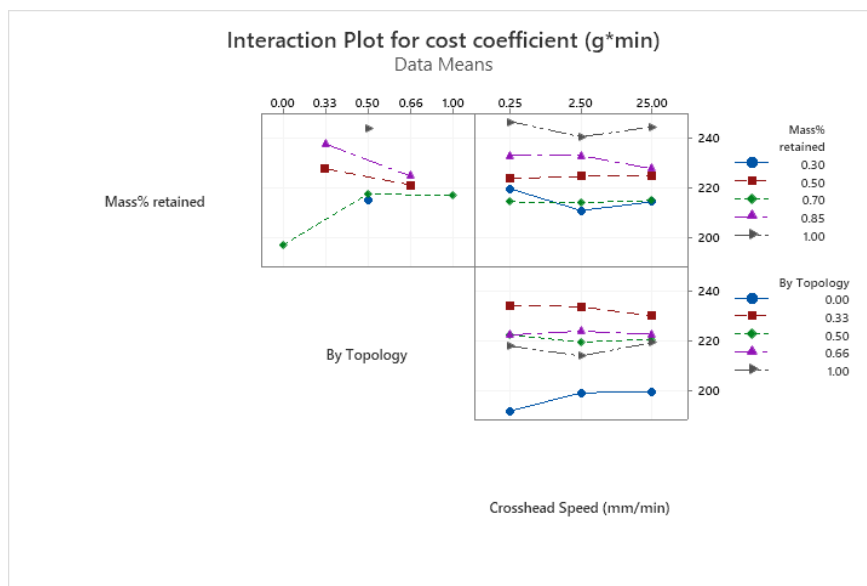


Figure 53 Interaction plot of cost-coefficient for Tensile

A 70% mass with 0:100 (topology: infill) corresponds to lowest cost coefficient. Although 30% mass in general is assumed to have lower cost since it needs comparatively less material but for 30% mass, we used 50:50 (topology: infill) combinations. That being said, time for manufacturing may increase to achieve a level of topology optimisation and hence a higher corresponding cost coefficient. That is why, when used only infill density for 70% mass, cost coefficient is lower than cost coefficient of 30% mass where a topology optimisation of 50% was used to achieve the level of mass reduction along-with 50% infill contribution. That can be a considerable future work for the cost model of FDM.

Finally, the residual assumptions are desirable for normality. We can see that in the probability and scatter plots below.

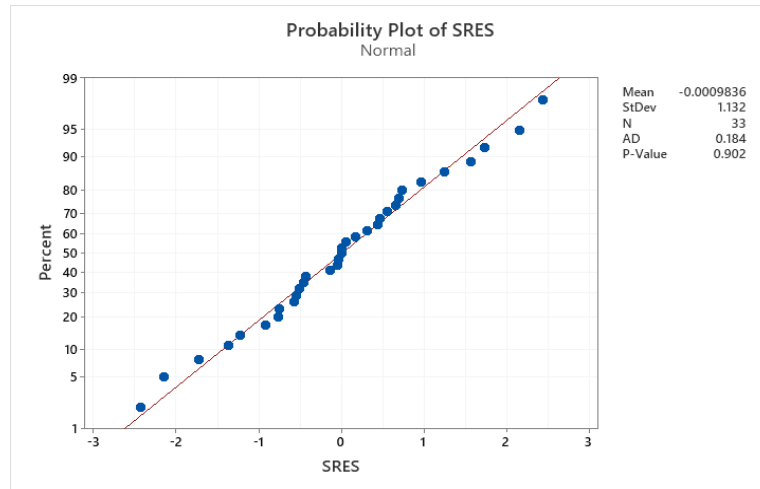


Figure 54 Probability plot of Tensile

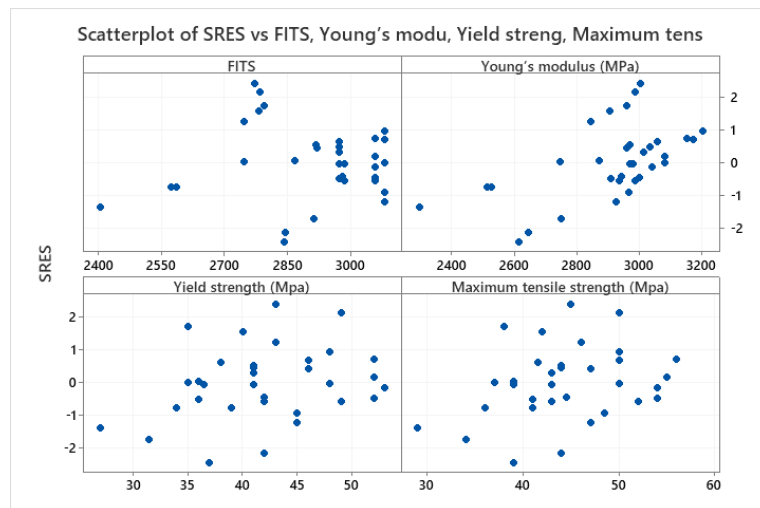


Figure 55 Scatter plot of SRES vs Fits, E, YS and Maximum tensile strength

The normality assumption cannot be rejected with a P-value greater than 0.05. The SRES belong to the interval $[-3;3]$ and thus we conclude that the model is validated.

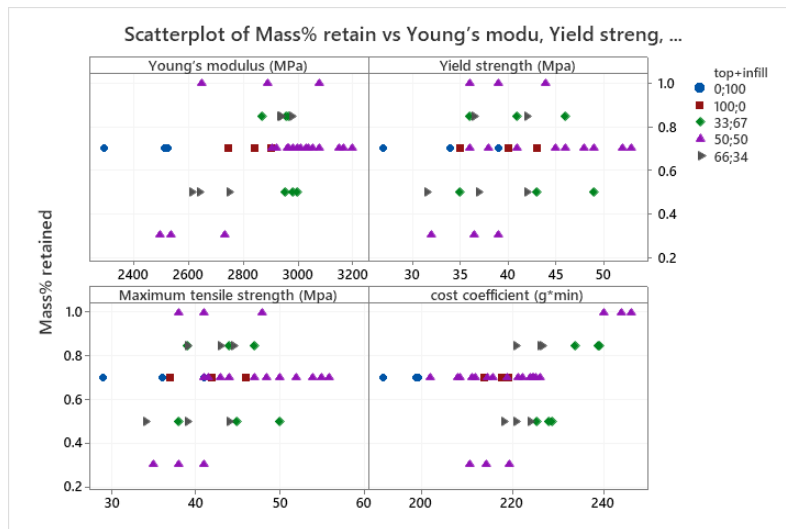


Figure 56 Scatterplot of mass vs E, YS, cost-coefficient, and maximum tensile strength

7. Conclusion

The aim of this work was to study the combined effects of topology optimisation and infill density of extrusion-based additive manufacturing parts; thereby reducing the mass with the objective of retaining the maximum strength. The variations of mass percentage were 100%, 85%, 70%, 50% and 30% while the combination of topology and infill density used for mass reduction were 67:33, 34:66 and 50:50, respectively.

For study purpose, bio-degradable PLA material was used, and additive manufacturing process was FDM. Desktop FDM machine Creality Ender-3 was used to manufacture the test samples. The topology optimisation was carried out before printing and the objective was to retain the maximum strength, while the infill density was set in Cura software for each sample just before printing command. The details of such software and procedures are presented in chapter 4.

Summarizing the results of experimental analysis, it can be concluded that the combined application of topology optimisation and infill density for mass reduction results in varying mechanical properties and cost for both compression and tension. Moreover, combining various levels results in varying responses for strength and cost and hence an optimised level exists.

It can be concluded for compression samples that the factors under study are significant, as shown in the ANOVA tables for each response. Moreover, these factors represent random main effects, and that interaction of topology optimisation and infill density is also significant. It can be seen from Fig 45 that various levels of combinations of topology and infill with varied mass percentages result differently on the responses but a mass reduction of 15% would be a good compromise for mechanical properties under study. We can also notice that this 15% reduction in mass had 66% contribution by topology optimisation and 34% by infill density. Moreover, the cost coefficient seems to have a very good compromise for 30% mass reduction for which the topology and infill density had 50% contribution each. Considering the mechanical performance and cost-effectiveness, however, we can find a good compromise at 85% mass with 66% topology optimisation. Moreover, crosshead speed of 25 mm/min is more evident for mechanical properties while it does not affect the cost, as shown in main effects plots Figure 35, 36, 37 and 38 for young's modulus, yield strength, maximum compression strength and cost, respectively.

In case of Tensile samples, on the basis of statistical analysis, it is observed that combining infill density and topology optimisation is a method for finding a compromise between strength and cost. For example, we can see from main effects plots of young's modulus (Fig 46), yield strength (Fig 47), maximum tensile strength (Fig 48), and cost-coefficient (Fig 49) that 70% mass results in better mechanical performance and cost-effectiveness. Similarly, from scatterplot (Fig 56) we can conclude that 70% mass is a good compromise between the strength and cost. Moreover, for overall mechanical performance and cost-effectiveness, this 30% mass reduction would be beneficial with 50% contribution of topology optimisation and 50% contribution of infill density.

There is still huge potential of future work in this domain and more combinations of topology and infill with varying levels of mass reductions can be exploited and explored with interesting outcomes by taking various interactions of these factors. Similarly, more materials can be tested apart from PLA with more shapes and mechanical tests such as bending.

8. References

- [1] Fuda Ning a, Weilong Cong a, Jingjing Qiu b, Junhua Wei b, Shiren Wang, “Additive manufacturing of carbon fiber reinforced thermoplastic composites using fused deposition modelling”, *Composites Part B* 80, (2015) 369-378, 80
DOI: 10.1016/j.compositesb.2015.06.013
- [2] Kedarnath Rane, Matteo Strano, “A comprehensive review of extrusion-based additive manufacturing processes for rapid production of metallic and ceramic parts”, *Adv. Manuf.* (2019) 155–173, 7(2) DOI:10.1007/s40436-019-00253-6
- [3] Clemens Lieberwirth, Arne Harder and Hermann Seitz, “Extrusion Based Additive Manufacturing of Metal Parts”, *Journal of Mechanics Engineering and Automation*, (2017), 7(2) DOI:10.17265/2159-5275/2017.02.004
- [4] Doubrovski, Z. (2016), “Design Methodology for Additive Manufacturing: Supporting Designers in the Exploitation of Additive Manufacturing Affordances”,
DOI:10.4233/uuid:d4214bb0-5bfd-43fe-af42-01247762b661
- [5] Dominik Deradjat, Dr. Tim Minshall, “Implementation of Rapid Manufacturing for Mass Customisation”, DOI:10.17863/CAM.4528
- [6] Adil Khan, Design and Characterizing of an Innovative Acoustic Resonator,
DOI:10.13140/RG.2.1.3107.3364
- [7] Marianna Rinaldi, Tommaso Ghidini, Federico Cecchini, Ana Brandao, Francesca Nanni, “Additive layer manufacturing of poly (ether ether ketone) via FDM”,
Composites Part B Engineering (2018) 162–172, 145
DOI: 10.1016/j.compositesb.2018.03.029
- [8] Jonathan Shindler, The Optimisation of 3D Printed Components.
<https://jamesgopsill.github.io/StudentProjects/projects/2014/CustomInfill/report.pdf>
- [9] Jun Wu, Niels Aage, Rudiger Westermann, Ole Sigmund, “Infill Optimization for Additive Manufacturing—Approaching Bone-like Porous Structures”, February 2018
IEEE Transactions on Visualization and Computer Graphics 24(2):1127-1140
DOI:10.1109/TVCG.2017.2655523
- [10] Huangchao Yu, Huajie Hong, Su Cao and Rafiq Ahmad, “Topology Optimization for Multipatch Fused Deposition Modeling 3D Printing”, *Applied Sciences (Switzerland)*, (2020), 10(3), DOI: 10.3390/app10030943
- [11] Joseph T. Belter, Aaron M. Dollar, “Strengthening of 3D Printed Fused Deposition Manufactured Parts Using the Fill Compositing Technique”, *PLoS ONE*, (2015), 10(4)
DOI: 10.1371/journal.pone.0122915
- [12] Nicol`o Manfredi, “Lightweight structures: topology optimization and 3D printing”,
<http://www-2.unipv.it/compmech/dissertations/manfredi.pdf>

- [13] David Moises Baca Lopez and Rafiq Ahmad, “Tensile Mechanical Behaviour of Multi Polymer Sandwich Structures via Fused Deposition Modelling”, *Polymers*, (2020), 12(3), DOI: 10.3390/polym12030651
- [14] Svetlana Terekhina, Innokentiy Skorniyakov, Tatiana Tarasova and Sergei Egorov, “Effects of the Infill Density on the Mechanical Properties of Nylon Specimens Made by Filament Fused Fabrication”, *Technologies*, (2019), 57, 7(3)
DOI: 10.3390/technologies7030057
- [15] Jan Podroužek, Marco Marcon, Krešimir Nincevic and Roman Wan-Wendner, “Bio Inspired 3D Infill Patterns for Additive Manufacturing and Structural Applications”, *Materials*, (2019), 12(3), DOI: 10.3390/ma12030499
- [16] Vladimir E. Kuznetsov, Azamat G. Tavitov, Oleg D. Urzhumtsev, Mikhail V. Mikhailin and Alexey N. Solonin, “Design and Fabrication of Strong Parts from Poly (Lactic Acid) with a Desktop 3D Printer: A Case with Interrupted Shell”, *Polymers*, (2019), 11(5) DOI: 10.3390/polym11050760
- [17] D. Brackett, I. Ashcroft, R. Hague, “TOPOLOGY OPTIMIZATION FOR ADDITIVE MANUFACTURING”
<https://sffsymposium.engr.utexas.edu/Manuscripts/2011/2011-27-Brackett.pdf>
- [18] Jikai Liu & Andrew T. Gaynor & Shikui Chen & Zhan Kang & Krishnan Suresh & Akihiro Takezawa & Lei Li & Junji Kato & Jinyuan Tang & Charlie C. L. Wang & Lin Cheng & Xuan Liang & Albert. C, “Current and future trends in topology optimization for additive manufacturing”, *Structural and Multidisciplinary Optimisation*, (2018), 2457–2483, 57(6)
DOI: 10.1007/s00158-018-1994-3
- [19] Anders Clausen, Niels Aage, Ole Sigmund, “Exploiting Additive Manufacturing Infill in Topology Optimization for Improved Buckling Load”, *Engineering*, (2016) 250–257, 2(2), DOI: 10.1016/J.ENG.2016.02.006
- [20] S. Garzon-Hernandez, D. Garcia-Gonzalez, A. Jérusalem, A. Arias, “Design of FDM 3D printed polymers: An experimental-modelling methodology for the prediction of mechanical properties”, *Materials and Design*, (2020), 188
DOI: 10.1016/j.matdes.2019.108414
- [21] Sandra Petersmann, Martin Spoerk, Philipp Huber, Margit Lang, Gerald Pinter, and Florian Arbeiter, “Impact Optimization of 3D-Printed Poly (methyl methacrylate) for Cranial Implants”, *Macromolecular Materials and Engineering*, (2019), 304(11)
DOI: 10.1002/mame.201900263
- [22] Amir M. Mirzendehtdel, Behzad Rankouhi, Krishnan Suresh, “Strength-Based Topology Optimization for Anisotropic Parts”, November 2017,
DOI:10.1016/j.addma.2017.11.007
- [23] J. Giannatsis, K. Sofos, V. Canellidis, D. Karalekas & V. Dedoussis, “Investigating the influence of build parameters on the mechanical properties of FDM parts”, *Laboratory*

of Advanced Manufacturing Technologies & Testing, Dept. of Industrial Management and Technology, University of Piraeus, Greece

- [24] Tomas Zegard, Glaucio H. Paulino, “Bridging topology optimization and additive manufacturing”, *Structural and Multidisciplinary Optimization*, (2016), 175–192, 53(1) DOI: 10.1007/s00158-015-1274-4
- [25] Ismail Durgun, Rukiye Ertan, “Experimental investigation of FDM process for improvement of mechanical properties and production cost”, *Rapid Prototyping Journal*, (2014), 20(3) DOI: 10.1108/RPJ-10-2012-0091
- [26] Flavio S. Fogliatto, Giovani J.C. da Silveira, Denis Borenstein, “The mass customization decade: An updated review of the literature”, *Int. J. Production Economics*, 138 (2012) 14-25, DOI.org/10.1016/j.ijpe.2012.03.002
- [27] G. Costabile, M. Fera, F. Fruggiero, A. Lambiase, D. Pham, “Cost models of additive manufacturing: A literature review”, *International Journal of Industrial Engineering Computations*, 8 (2017) 263-282 DOI: 10.5267/j.ijiec.2016.9.001